Towards retrofitting integrated gasification combined cycle (IGCC) power plants with solid oxide fuel cells (SOFC) and CO_2 capture

A thermodynamic case study

Thallam Thattai, A.; Oldenbroek, V.; Schoenmakers, L.; Woudstra, T.; Purushothaman Vellayani, A.

DOI
10.1016/j.applthermaleng.2016.11.167

Publication date
2017

Document Version
Final published version

Published in
Applied Thermal Engineering

Applied Thermal Engineering 114 (2017) 170–185

Contents lists available at ScienceDirect

Applied Thermal Engineering

journal homepage: www.elsevier.com/locate/apthermeng

Research Paper

Towards retrofitting integrated gasification combined cycle (IGCC) power plants with solid oxide fuel cells (SOFC) and CO_2 capture – A thermodynamic case study

A. Thallam Thattai [a,*], V. Oldenbroek [a], L. Schoenmakers [b], T. Woudstra [a], P.V. Aravind [a]

[a] Process & Energy Laboratory, Delft University of Technology, Leeghwaterstraat 39, 2628CB Delft, The Netherlands
[b] Nuon Vattenfall Buggenum, Roermondseweg 55, 6081NT Haelen, The Netherlands

HIGHLIGHTS

- Principal case study for retrofitting solid oxide fuel cells in large power plants.
- Model development based on previously experimentally validated models.
- Process is feasible to retrofit up to 40 MW_e SOFC modules and partial CO_2 capture.
- Full scale SOFC and CO_2 capture requires major process redesign and modifications.
- Exergy analysis indicates high efficiency improvement with SOFC integration.

ARTICLE INFO

Article history:
Received 27 July 2016
Revised 30 September 2016
Accepted 22 November 2016
Available online 24 November 2016

Keywords:
IGCC
SOFC
Retrofit
CO_2 capture
Exergy

ABSTRACT

This article presents a detailed thermodynamic case study based on the Willem-Alexander Centrale (WAC) power plant in the Netherlands towards retrofitting SOFCs in existing IGCC power plants with a focus on near future implementation. Two systems with high percentage (up to 70%) biomass co-gasification (based on previously validated steady state models) are discussed: (I) a SOFC retrofitted IGCC system with partial oxy-fuel combustion CO_2 capture (II) a redesigned highly efficient integrated gasification fuel cell (IGFC) system with full oxy-fuel CO_2 capture. It is concluded that existing IGCC power plants could be operated without major plant modifications and relatively high electrical efficiencies of more than 40% (LHV) by retrofitting SOFCs and partial oxy-combustion CO_2 capture. In order to apply full scale CO_2 capture, major process modification and redesign needs to be carried out, particularly in the gas turbine unit and heat recovery steam generator (HRSG). A detailed exergy analysis has also been presented for both the systems indicating significant efficiency improvement with the utilization of SOFCs. Additional discussions have also been presented on carbon deposition in SOFCs and biomass CO_2 neutrality. It is suggested that scaling up of the SOFC stack module be carried out gradually, synchronous with latest technology development. The thermodynamic analysis and results presented in this article are also helpful to further evaluate design challenges in retrofitted IGCC power plant systems for near future implementation, gas turbine part load behaviour, to devise appropriate engineering solutions and for techno-economic evaluations.

1. Introduction

Multiple initiatives and targets have been set in the European Union (EU) by the European Commission like Paris COP21 agreement [1], Roadmap 2050 [2], the 2030 framework for climate and energy [3], 20–20–20 climate and energy package [4] to mitigate greenhouse gas (GHG) related climate change in near future. Emission of GHG gases (mainly CO_2) from coal based power plants is a major contributor in the total GHG emission. Utilization of

Abbreviations: ASU, Air Separation Unit; CC, CO_2 capture; CCS, carbon capture and storage; CO_2, Carbon Dioxide; COS, carbonyl sulphide; EU, European Union; GCU, gas cleaning unit; GHG, greenhouse gas; GT, gas turbine; HRSG, heat recovery steam generator; HP, high pressure; H_2, hydrogen; HCN, hydrogen cyanide; IGCC, integrated gasification combined cycle; IGFC, integrated gasification fuel cell; IP, intermediate pressure; LHV, lower heating value (MJ/kg); LP, low pressure; SCGP, shell coal gasification process; SOFC, solid oxide fuel cell; ST, Steam Turbine; SGC, syngas cooler; VIGV, variable inlet guide vane; WGS, water gas shift; WAC, William Alexander Centrale.

* Corresponding author.
E-mail address: A.ThallamThattai@tudelft.nl (A. Thallam Thattai).

http://dx.doi.org/10.1016/j.applthermaleng.2016.11.167
1359-4311/

biomass as feedstock to produce electrical power offers a large potential to develop CO_2 neutral power plants [5–7]. Biomass based IGCC power plants (called BioIGCC) with CO_2 capture (CC) could be a potential solution for developing CO_2 negative power plants since the stored CO_2 originates from biomass while biomass absorbs CO_2 for its growth. With high CO_2 capture rates such plants can significantly contribute to mitigation of the energy system emissions [8]. However the utilization of CO_2 capture leads to a reduction in the net electrical/exergy efficiencies [9,10]. In order to boost electrical/exergy efficiencies the system could be improved by partially replacing highly irreversible processes like combustion with highly efficient electrochemical conversion [11].

The amount of biomass co-gasification is key to the CO_2-negative capabilities of power plants. The 253 MW_e Willem-Alexander Centrale (WAC), a now defunct integrated gasification combined cycle (IGCC) plant in Buggenum, The Netherlands has been previously operated with high percentage (over 70%) biomass co-gasification [12]. No other IGCC power plant in the world has been operated before with such high percentage of biomass co-gasification. With such a successful large scale experimental demonstration, it is very important to assess possibilities of developing high efficiency and CO_2 neutral power plants based on this demonstration.

Electrochemical conversion of syngas derived from coal/biomass gasification to produce power has been postulated as a more efficient route as compared to conventional combustion based gas turbine systems [13]. Solid oxide fuel cells (SOFC) are high efficiency (up to 70%) electrochemical devices which can be utilized to produce electrical power and heat. A significant number of modelling investigations have been carried out in the past by multiple research groups on the prospects of integrating SOFCs in coal based IGCC power plant systems. Park et al.[14,15] reported a comparative system study for pre-combustion and oxy-fuel combustion CO_2 capture in SOFC integrated IGCC plants concluding a better performance with oxy-fuel combustion CO_2 capture. Braun et al. [16] investigated the performance of a SOFC integrated coal based gasification power plant concept with a organic Rankine cycle power generator as the bottoming cycle. A quasi-2D finite volume SOFC model has been presented by Li et al. [17,18] as an aid for IGFC system analysis. Spallina et al.[19] have reported a novel coal based IGFC plant system design with CO_2 capture giving a net plant efficiency of about 47.5%. A zero-emission power plant concept was reported by Adams and Barton [20] by combining coal gasification with solid oxide fuel cells. They conclude that the use of SOFCs with unmixed anode and cathode exhausts makes the process inherently CO_2 capture friendly. A number of system and economic investigations have also been reported by the Department of Energy (DoE), USA assessing various configurations for coal based IGFC power plant designs [21–26]. Additional IGFC system concepts and designs have been presented by Ghezel-Ayagh et al. [27], Li et al. [28], Rudra et al. [29]. A comprehensive exergy and economic analysis on advanced coal based IGCC-CCS and IGFC-CCS was carried out by Siefert and Litster [30]. It can be seen that much research work on integrating SOFCs has been focussed on coal based IGCC power plant systems and all these studies present the design/performance of new systems focussed on long term implementation.

In the recent past, a few system investigations have also been reported on SOFC integration in IGCC power plants with biomass co-gasification. Jin et al. [31] conducted investigations on comparing the thermodynamic and economic performance of biomass based IGCC with and without SOFC integration. CO_2 capture was not considered in this study. They reported a net electrical efficiency of 47.1% for the bioIGCC-SOFC system. Paengjuntuek et al. [32] presented simulation results for an integrated biomass gasification fuel cell plant with a net energy efficiency of 69.38% (combined heat and power). Naraharisetti et al.[33] have reported a comparative study for a biomass based IGCC and IGFC with biomass and natural gas as fuel using multi-objective optimization (MOO). A detailed and comprehensive study has been reported by Sadhukhan et al. [34] with process simulation and methodology for the integrated design of biomass gasification fuel cell systems and comparison of these biomass gasification combined cycle systems. They identify process constraints and extreme operating conditions for the SOFC unit and the steam cycle. Literature review thus reveals that research on SOFC and CO_2 capture integration in coal/biomass based IGCC power plant systems has only been focussed on the design of new systems. There exists an absence in information available on the thermodynamic effects of retrofitting solid oxide fuel cells in existing IGCC power plants with CO_2 capture with a focus on near future implementation. Despite information available on retrofitting CO_2 capture in IGCC power plants [35,36], nothing has yet been reported concerning SOFC integration.

Retrofitting existing power plants marks a major step in evaluating novel technologies in terms of application in near future. With intensive global ongoing efforts [37,38] on developing kW scale fuel flexible SOFC stacks, research needs to be carried out in understanding and assessing challenges in retrofitting such SOFC stack modules in existing coal/biomass based IGCC power plants. In order to make choices to retrofit, it is of utmost importance to assess power plant off-design performance, required process modifications and operational boundaries based on the existing equipment in the power plant. Multiple challenges exist to retrofit syngas fed SOFCs in existing power plants like cost, process design, material availability, contaminant tolerance, carbon deposition [39]. However apart from challenges to be overcome in the SOFC module itself, it is also important to assess system/process constraints based on the existing equipment in the power plant.

Detailed system models can be effective tools to evaluate plant performance with alternative and safe operating conditions. Operation of the coal based WAC with 70% biomass co-gasification, SOFC and CO_2 capture can be considered as an off-design situation in the context of modelling studies. An off-design model analysis allows performance prediction due to change in the operating point of the system when compared to design case inputs and outputs. It is very important to understand the off-design plant performance based on experimentally validated models. Previous modelling studies on IGCC power plants rely on literature or small scale tests as a prime data source for the base case model development and reliability thus remains highly debatable. The authors have previously reported a thermodynamic study on WAC with detailed experimental model validation using coal [40] and high percentage (up to 70%) biomass co-gasification [12]. Based on these validated models, it has been decided to assess the thermodynamic performance and identify process constraints in the WAC plant when retrofitted with solid oxide fuel cells and oxy-fuel combustion CO_2 capture technology.

This article presents an alternative approach towards introducing SOFCs in IGCC power plants, by suggesting a step wise scale up strategy. For the first time in scientific literature, a reliable steady state model based study is presented towards retrofitting SOFCs and partial oxy-fuel combustion CO_2 capture in existing IGCC power plants (with up to 70% biomass co-gasification). Focus has been given to identify bottleneck thermodynamic situations and process modifications. Detailed thermodynamic models (based on previously experimentally validated models [40,12]) are discussed for two systems: (i) a SOFC- partial oxyfuel combustion CO_2 capture retrofitted IGCC system based on WAC plant design. The system involves the use of a split stream of syngas after gas cleaning in an SOFC stack unit to develop additional power. (ii) A redesigned highly efficient and fully integrated gasification fuel

cell (IGFC) system with full oxy-fuel combustion CO_2 capture based on the existing WAC gasifier and gas cleaning unit (GCU); wherein all syngas produced in the gasifier is fed to the SOFC unit and consequently to the HRSG and CO_2 capture unit. For both systems, detailed off-design models have developed utilizing 70% steam exploded wood pellets and 30% coal (energy based) as feedstock. The methodology and conclusions are however equally applicable to coal based retrofitted IGCC systems. A detailed exergy analysis has also been presented for both the systems indicating the efficiency improvement with the utilization of SOFCs. Additional discussions have also been presented on carbon deposition in SOFCs and biomass CO_2 neutrality.

2. Plant overview and case description

The Willem-Alexander Centrale (WAC) has been a key demonstration plant for coal based IGCC technology. The power plant was constructed in 1989 by Demkolec (defunct company now), a consortium of Dutch power producers [41]. The plant design is based on the Shell Coal Gasification Process (SCGP) in which pulverized fuel mix is converted to synthesis gas (syngas) under sub-stoichiometric conditions in a dry feed slagging entrained flow gasifier at elevated temperatures between 1500 and 1800 °C. In the recent past, the power plant has also been operated with high percentage (over 70%) biomass co-gasification [12]. A detailed description of the power plant can be found in our previous articles [40,12].

Table 1 shows the definition for various cases considered in this study. The approach is to first investigate the system when retrofitted with a smaller SOFC stack module; the combined cycle still being the largest power producer. This represents the SOFC-CC Retrofit STEX case. The second case with a large SOFC stack module and full CO_2 capture i,e the IGFC-CC STEX case has been selected to identify the major process constraints and redesign necessary to scale up towards a full integrated IGFC power plant with CO_2 capture. STEX represents the previously reported [12] experimentally validated case for the co-gasification test at WAC with 70% steam exploded woodpellets. This reference case is presented to compare the performance of the SOFC-CC Retrofit STEX and IGFC-CC STEX cases.

2.1. SOFC-CC Retrofit STEX (with partial CO_2 capture)

Fig. 1 illustrates the primary components of the proposed retrofitted WAC system in a process flow diagram. Coal and biomass mixture is pulverized and blown into the gasifier and the produced syngas is cooled and cleaned to remove HCN/COS and sulphur based compounds (H_2S). A part of the clean syngas is then extracted, preheated and fed to the SOFC stack. The remaining syngas is diluted with N_2, saturated with water vapour and fed to the gas turbine combustor. Cathode air for the SOFC stack is extracted also from the air compressor. Partial CO_2 capture is then employed. The unconverted syngas at the SOFC stack anode outlet is combusted with an oxy-fuel combustor with pure O_2 (95% vol from ASU) to produce a gas mixture primarily consisting of CO_2 and H_2O. This gas mixture is then cooled to condense out moisture to obtain pure CO_2. A multistage compressor with intercooling is then employed to compress CO_2 to the desired storage pressure. Depleted cathode outlet air from the SOFC stack is fed to the gas turbine (GT) combustor. The flue gas from the GT combustor is guided through a gas turbine expander generating power and further through a heat recovery steam generator (HRSG). The generated steam in the HRSG is then expanded in steam turbines for additional power generation.

Table 1
Case definition.

Case	Description
STEX [12] (no CC)	IGCC system based on WAC plant design with a fuel consisting of 70% steam exploded woodpellets and 30% Columbian coal
SOFC-CC Retrofit STEX (partial CC)	STEX case based on WAC plant design with retrofitted SOFC stack and partial oxy-combustion CO_2 capture. The SOFC stack is not the main power producing unit.
IGFC-CC STEX (full CC)	STEX case in a redesigned IGFC configuration with full oxy-combustion CO_2 capture based on WAC gasifier and gas cleaning unit (GCU) design. The SOFC stack is the main power producing unit. The original GT is replaced with an air expander

2.2. IGFC-CC STEX (with full CO_2 capture)

The second system presented in this article consists of a redesigned (but based on WAC gasifier and GCU design) IGFC power plant system with full oxy-combustion CO_2 capture. Fig. 2 shows the process flow diagram for this system. The system consists of an identical gasifier, syngas cooler and gas cleaning unit as the retrofitted system described in the previous subsection. All the clean syngas obtained after gas cleaning is fed as fuel to the SOFC stack unit. As bulk of the clean syngas is converted through electrochemical oxidation in the SOFC stack module instead of the GT combustor, this system does not require the N_2 dilution and saturation unit after the gas cleaning unit (GCU). N_2 dilution and water vapour saturation is utilized mostly to limit high combustion temperatures and NO_x emissions [13]. Hence the co-produced N_2 in the ASU is vented to the atmosphere or can be considered as a co-product. The SOFC stack replaces the combustion chamber of the gas turbine. A pressurized SOFC stack is considered for maximizing efficiency. To carry out full CO_2 capture, the anode outlet gas is then directed to an oxy-fuel combustor where the remaining fuel is combusted with pure oxygen (95%) at near stoichiometric conditions. The oxygen required for the oxy-fuel combustor is obtained from the existing ASU. The outlet gas from the oxy-combustor mainly consisting of CO_2 and H_2O is cooled to condense out moisture to obtain pure CO_2. The thermal energy in the outlet gas is recovered partly in a newly designed pressurized HRSG. An identical CO_2 cooling and compression process is then utilized as in the retrofitted system. The cathode outlet air stream from the SOFC stack, depleted in O_2 content, cannot be utilized in the combustor as this will lead to undesirable nitrogen in the captured CO_2 stream. Hence the original WAC flue gas GT expander is replaced with an air expander. This expanded air stream is cooled in the HRSG to generate additional steam and subsequently vented into the atmosphere via the stack.

3. Modelling approach and description

Cycle-Tempo, a Fortran based in-house modelling software package [42], is utilized for steady-state model development. The software has a system component library which can be assembled and modified by applying appropriate operating parameters to build a custom-made system configuration. Thermodynamic and required transport properties have been obtained from the in-house software library FluidProp [43].

The coal-biomass feedstock mixture composition is shown in Table 2. This represents the composition of the fuel mix fed to the gasifier after the drying operation. A high ash content coal has been chosen in order to maintain sufficient slag that helps cover and protect the gasifier membrane wall. Ash consists of various compounds but mainly quartz (SiO_2), hematite (Fe_2O_3) and

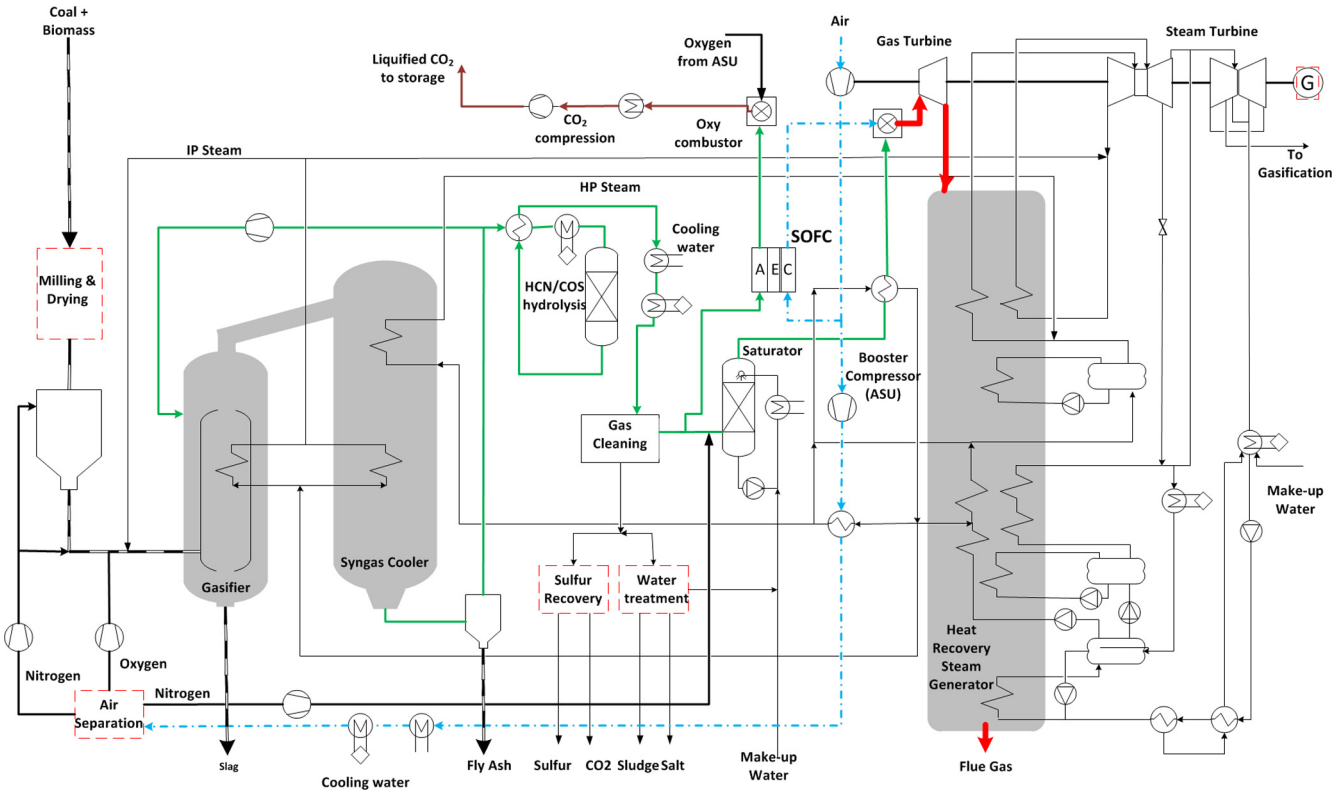

Fig. 1. Process flow diagram for SOFC-CC Retrofit STEX system – red dotted blocks have not been modelled, brown streams represent CO_2 flow. (For interpretation of the references to colour in this figure legend, the reader is referred to the web version of this article.)

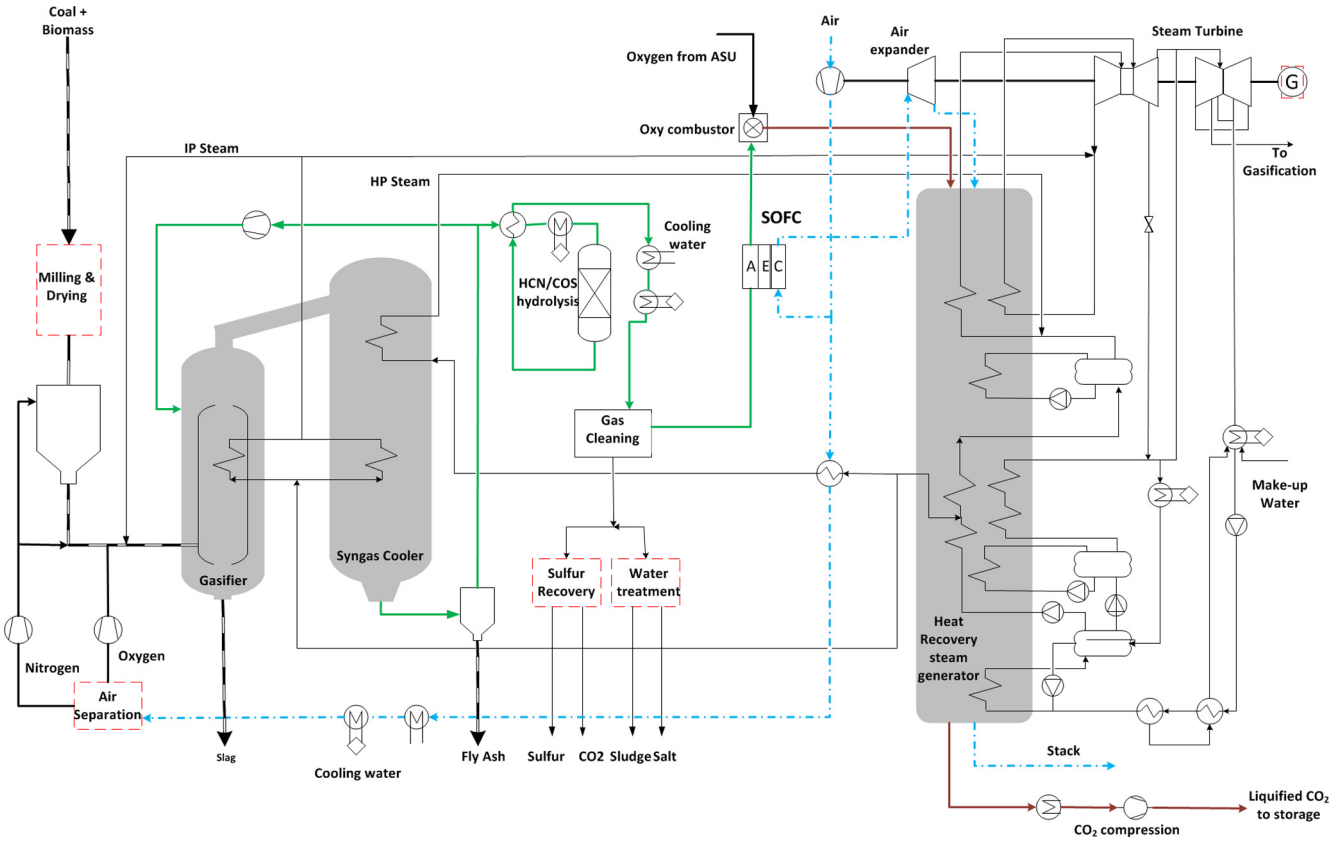

Fig. 2. Process flow diagram for IGFC-CC STEX system – red dotted blocks have not been modelled. (For interpretation of the references to colour in this figure legend, the reader is referred to the web version of this article.)

Table 2
Gasifier input fuel mix composition.

Component	Al_2O_3	C	Cl	Fe_2O_3	H	H_2O	N	O	S	SiO_2	SO_3
(wt%)	2.23	51.75	0.01	1.18	4.45	2.00	0.80	27.72	0.43	9.09	0.34

aluminium oxide (Al_2O_3). These three compounds with highest mole fraction are included in the fuel composition. The fuel mix contains negligible amount of limestone. The ultimate and proximate analysis of the coal and biomass feedstock is shown in Table 3.

3.1. Off-design modelling and description

Operation of retrofitted WAC (originally designed for coal) with 70% biomass co-gasification and SOFC-CO_2 capture can be considered as an off-design case for all equipment (except SOFC and CO_2 capture unit) in the context of modelling studies. Cycle Tempo offers possibility to model off-design behaviour of several components like turbines, heat exchangers, flash heaters, condensers and pipes.

- **Turbines**: Off-design calculations are possible for all types of turbines in Cycle Tempo. Traupel's formulae (a refinement of Stodola's cone law) are used to calculate off-design performance based on design case values [42,44,45]. Design case values of pressures, flow rates and specific volumes are needed to compute the off-design turbine inlet pressure. Eq. (1) shows the Traupel's formulae considered in Cycle-Tempo to calculate the off-design inlet pressure **p** from the specific volume **v**, mass flow rate **m** and the polytropic exponent **n**. Subscript α represents the inlet and ω the outlet. Sub-subscript **o** represents the design case value.

$$\frac{m}{m_o} = \frac{p_\alpha}{p_{\alpha_o}} \left\{ \frac{p_{\alpha_o} v_{\alpha_o}}{p_\alpha v_\alpha} \right\}^{1/2} \left[\frac{1 - \left(\frac{p_\omega}{p_\alpha}\right)^{\frac{n+1}{n}}}{1 - \left(\frac{p_{\omega_o}}{p_{\alpha_o}}\right)^{\frac{n_o+1}{n_o}}} \right]^{1/2} \tag{1}$$

Applying Poisson's formula:

$$p v^n = \text{constant} \tag{2}$$

$$p_\alpha = p_\omega \left\{ 1 + (k_o m)^2 \frac{v_\omega}{p_\omega} \right\}^{\frac{n}{n+1}} \tag{3}$$

$$k_o = \frac{1}{m_o} \left\{ \frac{p_{\omega_o}}{v_{\omega_o}} \right\}^{1/2} \left[\left(\frac{p_{\alpha_o}}{p_{\omega_o}} \right)^{\frac{n_o+1}{n_o}} - 1 \right]^{1/2} \tag{4}$$

Table 3
Raw fuel composition and lower heating values for Columbian coal and steam exploded woodpellets.

	Columbian coal	Steam exploded pellets
Ultimate Analysis		
C	50.06	54.20
H	3.36	5.97
N	1.32	0.20
O	8.98	39.11
S	0.99	0.01
Cl	0.015	0.004
Ash	35.27	0.50
Proximate Analysis		
Ash, %	35.27	0.50
Moisture, %	13.38	5.06
Fixed Carbon, %	25.70	19.17
Volatile Matter, %	25.65	75.27
LHV, MJ/kg	20.00	19.32

k_o is only dependent on the design case values and is therefore a constant. The polytropic constant is derived based on Eq. (2) for design and off-design conditions. The use of Eq. (3) to predict off-design pressure for steam turbines is well justified [45] but the equation is modified for the gas turbine employing the equation for subcritical nozzle flow as shown in Eq. (5).

$$\frac{m}{m_o} = \frac{p_\alpha}{p_{\alpha_o}} \left\{ \frac{p_{\alpha_o} v_{\alpha_o}}{p_\alpha v_\alpha} \right\}^{1/2} \left[\frac{\left(\frac{p_\omega}{p_\alpha}\right)^{\frac{2}{n}} - \left(\frac{p_\omega}{p_\alpha}\right)^{\frac{n+1}{n}}}{\left(\frac{p_{\omega_o}}{p_{\alpha_o}}\right)^{\frac{2}{n}} - \left(\frac{p_{\omega_o}}{p_{\alpha_o}}\right)^{\frac{n+1}{n}}} \right]^{1/2} \tag{5}$$

- **Heat exchangers**: Cycle Tempo calculates the off-design heat transfer capacity UA (W/K) from the design case $(UA)_o$ value and mass flow rate (m_o) which mostly influences the overall heat transfer coefficient. The off-design heat transfer rate is calculated as shown in Eq. (6). This formula should not be used for discontinuous temperature profiles.

$$UA = (UA)_o \cdot \left(\frac{m}{m_o} \right)^{0.8} \tag{6}$$

- **Flash heaters**: Off-design calculations for flash heaters are not scaled with the UA-value since a reliable UA-value cannot be established for heat exchange between media showing phase changes. Depending on the ratio between the off-design mass-flow rate and the design mass-flow rate, temperature differences are adapted according to performance curves [46].
- **Condensers**:The heat exchanging area is an input to calculate the off-design behaviour in Cycle-Tempo. With a known heat transfer and cooling water temperatures, the overall heat transfer in the off-design case will be calculated according to instructions as stated in the VDI Heat Atlas [47].
- **Other components**: Other major components of the system include the gasifier and combustor. Off-design modelling of these components demands knowledge and an accurate model for heat release/heat transfer in these components and variation in the gasification/combustion chemistry. For example, the heat absorbed by the gasifier walls/the heat transferred to the gasifier cooling system etc. This heat depends on the thickness of the slag layer and models to predict this are very complex to develop and not readily available. Also due to high operating temperatures ($T_{gasifier}$ > 1500 °C, T_{comb} = 1050 °C), it is reasonable to assume a constant operating profile for these components.

A detailed description on the off-design calculation procedure in Cycle-Tempo can be found in our previous article [12]. Input data for the gasifier, gas cleaning and saturation, gas turbine and steam turbine units remain unchanged. This input data can be obtained from our previous articles [40,12]. The gas turbine combustor has been modelled with air-fuel equivalence ratio (λ) of 2.0 and a combustor outlet temperature of 1575 °C, assuming no NO_x formation at these conditions. The main input parameters only for the SOFC unit and oxy-fuel combustion CO_2 capture unit are presented in this section.

Table 4 shows the main input parameters (assumed) used in the Cycle-Tempo SOFC model. The SOFC operating conditions, geometry and materials have been chosen on a generic basis for standard performance. Cycle-Tempo offers an in-built SOFC model based on

Table 4
Cycle-tempo SOFC model – assumed design parameters, geometry and materials.

Assumed design conditions	
Operating cell temperature, °C	900.00
Current density, A/m^2	2500.00
Fuel utilization, %	0.85
Equivalent resistance (R_{eq}), Ω m^2	5.00e−5
Anode & Cathode inlet gas temperature, °C	850.00
Pressure loss (anode and cathode), bar	0.05
DC to AC conversion efficiency, %	95.00
Recirculation compressor isentropic efficiency, %	0.85
Geometry assumptions	
Design	Planar
Operating mode	Direct internal reforming (DIR)
Anode material	Ni/GDC
Cathode material	LSM-YSZ
Electrolyte material	YSZ
Support	Electrolyte

thermodynamic and electrochemical considerations. The model calculates the active area, voltage, current and the electrical power [46]. As the first step, an equilibrium calculation is carried out based on the inlet fuel (anode) composition, specified reaction temperature and pressure. A calculation procedure is then carried out to calculate other electrochemical parameters. The reversible voltage is calculated with the Nernst equation(Eq. (7)) assuming that only H_2 is electrochemically oxidized:

$$E_x = E^0 + \frac{R \cdot T}{2 \cdot F} \ln \left\{ \frac{{y_{O_2,c}}^{1/2} \cdot y_{H_2,a}}{y_{H_2O,a}} \cdot p_{cell}^{1/2} \right\} \quad (7)$$

E^0 is the standard reversible voltage for hydrogen, that only depends on the temperature, and is calculated from the change in the Gibbs energy ΔG. F is the Faraday constant, R is the universal gas constant and T is the operating cell/stack temperature. $y_{O_2,c}$ represents the mole fraction of oxygen on the cathode side, $y_{H_2,a}$ is the mole fraction of hydrogen in the anode fuel stream and $y_{H_2O,a}$ represents the mole fraction of water vapour on the anode side. p_{cell} is the cell/stack operating pressure. The actual operating voltage V_{cell} and the current I_{cell} is calculated as in Eqs. (8) and (9) respectively:

$$V_{cell} = E_x - \Delta V_x \quad i_x = \frac{\Delta V_x}{R_{eq}} \quad (8)$$

$$I_{cell} = \frac{U_f \cdot \phi_{m,a,in}}{M_{mol,a}} \cdot (y^0_{H_2} + y^0_{CO} + y^0_{CH_4}) \cdot 2F \quad (9)$$

ΔV_x represents the overpotentials/losses in the SOFC. The current density (i_x) is proportional to the voltage loss by analogy with Ohm's law. R_{eq} is the equivalent cell/stack resistance. U_f is the fuel utilization of the SOFC stack, $\phi_{m,a,in}$ is the mass flow rate of inlet fuel to the anode and $M_{mol,a}$ is the molar mass of the anode inlet fuel. Mass transport of O_2 from the cathode side is also calculated based on the current. Use of numerical subroutines is made to calculate these quantities over the cell. More detailed information on the calculation procedure can be found in the Cycle-Tempo technical manual [46].

The oxy-combustion CO_2 capture process has been modelled considering maximum heat integration in the system and high CO_2 purity. The main input parameters for the CO_2 capture model have been tabulated in Table 5. A 2 stage compression process with intercooling is utilized to compress the pure CO_2 stream. Cooling water available at around 12 °C is used for intercooling. In order to minimize the use of cooling water, heat from the capture unit is utilized to generate low pressure steam, which is subsequently used for condensate preheating. A total pressure drop of 2.5 bar is assumed for the cooling water system.

Table 5
Input parameters – oxy-combustion CO_2 capture.

Parameter	Value
CO_2 final discharge pressure, bar	150.00
CO_2 discharge temperature, °C	30.00
CO_2 compressor isentropic efficiency, %	80.00
Oxy-combustor reaction pressure, bar	10.75
Oxy-combustor reaction temperature, °C	1050.00
Oxy-combustor pressure drop, bar	0.27
Cooling water pump isentropic efficiency, %	65.00
Cooling water temperature difference, °C	5.00

Fig. 3 shows the simplified Cycle-Tempo model scheme for the SOFC-CC Retrofit STEX case. The SOFC unit and the partial oxy-combustion CO_2 capture unit have not been modelled in off-design mode as these are newly sized equipment added to the WAC system. In the SOFC unit, anode and cathode off-gas recirculation is utilized to maximize stack performance. Previous studies have indicated that utilization of anode/cathode off-gas recirculation facilitates improved stack performance also considering syngas internal reforming within the stack [48]. The hot flue gas from the oxy-fuel combustor is cooled down to 780 °C and preheat air fed into the cathode. Subsequent cooling of the flue gas is achieved by preheating the clean syngas stream to 750 °C. The flue gas is then passed through the CO_2 capture and compression unit. The cathode outlet gas is partially cooled down to preheat air before being sent to the gas turbine combustor. Two dummy heat exchangers are used to calculate the anode and cathode recycle flows. The HRSG design is largely based on the original WAC HRSG design. This has just been shown in the scheme with a single heat exchanger to maintain clarity. A detailed layout and design of the HRSG can be found in our previous article [12].

Fig. 4 shows the simplified Cycle-Tempo model scheme for the IGFC-CC STEX case. In this case, all equipment downstream the gas cleaning unit i,e SOFC, CO_2 capture unit, HRSG, air expander and steam turbine cycle are not modelled in off-design mode as they are newly designed. The inlet syngas fuel to the SOFC anode is preheated to 750 °C with flue gas from the oxy-fuel combustor. The HRSG involves the use of expanded air and flue gas (from oxy-fuel combustor) to generate HP, IP and LP steam. An integrated process is utilized where flue gas is utilized in the HP economizer, HP evaporator and IP superheater; while the expanded air is used in the LP evaporator and LP superheater. The cooled air is then used to preheat syngas and finally discharged to the atmosphere. Auxilliary load for both cases mainly comprises of power required for N_2 and O_2 compression in the ASU, fuel milling, power required in pumps, tracing and other miscellaneous power requirements. A detailed explanation on the constituents of the auxilliary load can be found in our previous article [12]. In addition, in both the cases, power is required for CO_2 compression in the CO_2 capture unit. This has also been included in the calculation of the total auxilliary load.

4. Results & discussion

The off-design performance of the SOFC-CC Retrofit STEX system and the IGFC-CC STEX system has been evaluated by analyzing operating parameters and gas compositions at various locations. Table 6 shows the model results for the SOFC-CC Retrofit STEX case with a comparison to the STEX case. As it can be seen the thermal input to the gasifier has been kept constant in order to make the comparison. The off-design system performance of the existing equipment (gasifier, SGC and syngas cleaning unit) remains almost

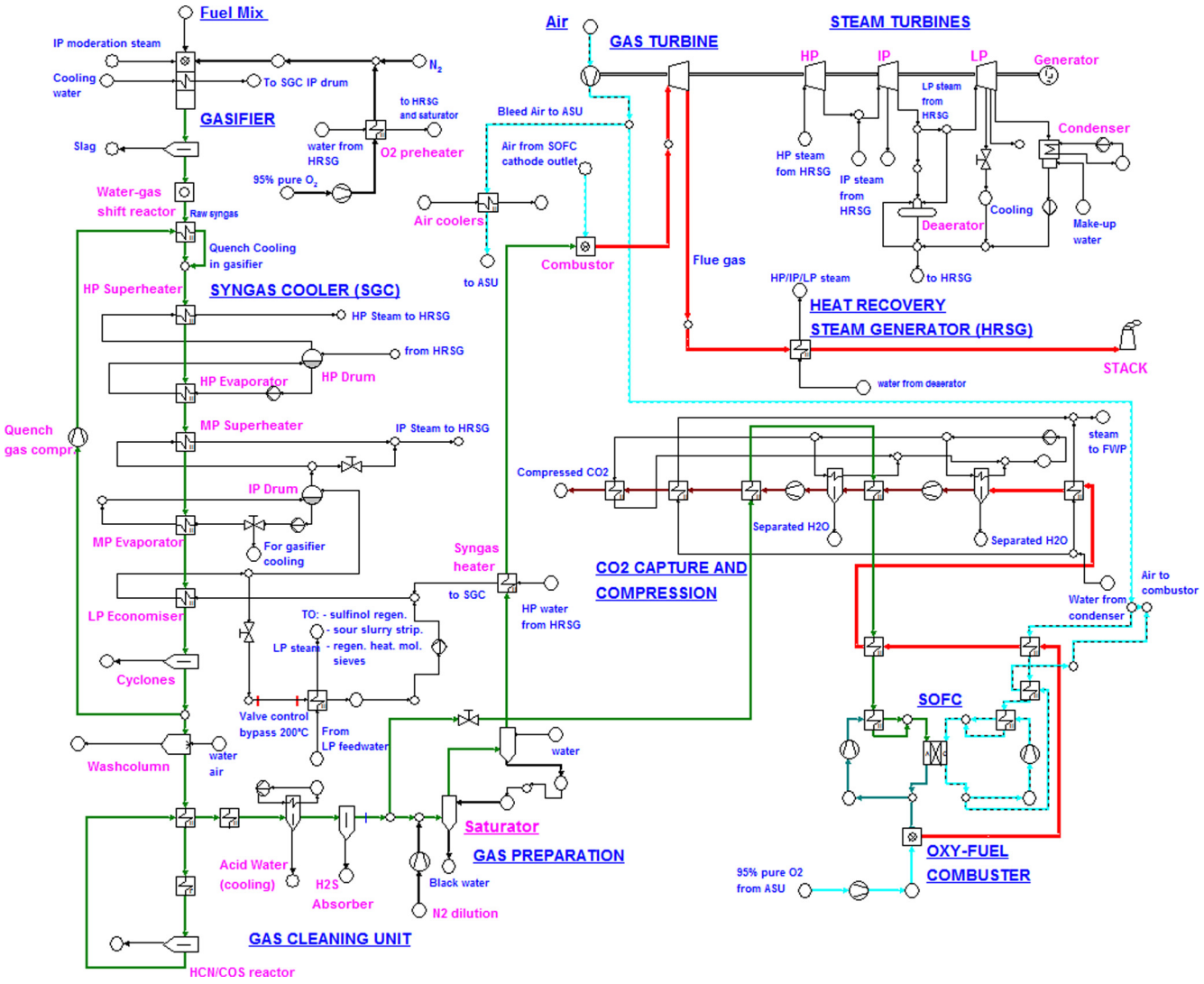

Fig. 3. Simplified process scheme for SOFC-CC Retrofit STEX (partial CO_2 capture) case – green streams represent syngas flow, red streams represent flue gas and blue streams represent air flow. Streams indicating detailed process/heat integration have been excluded to maintain clarity. (For interpretation of the references to colour in this figure legend, the reader is referred to the web version of this article.)

unchanged as seen from the table. A slightly higher temperature is used in the saturator. The syngas flow to the N_2 dilution and saturator is smaller in comparison to the STEX case due to a split stream of syngas fed to the SOFC. Consequently, the N_2 flow for dilution is decreased to 33 kg/s (A minimum flow rate of 33.0 kg/s N_2 dilution flow is obligatory for the ASU molecular sieves regeneration). Due to the syngas split stream to the SOFC, there is 28% reduction in the flue gas mass flow rate to the HRSG. This results in a lower steam production (HP/IP/LP) in the HRSG compared to the STEX case as a result of lower heat available in the HRSG.

The air mass flow rate is calculated in the model based on the requirements in the GT combustor and ASU. The discharge pressure from the air compressor is also calculated based on the integrated gas turbine cycle. An important observation from the results is the 18% lower air compressor discharge pressure in the SOFC-CC Retrofit STEX compared to the STEX case. The oxygen demand in the retrofitted plant is even higher than the STEX case, due to additional O_2 requirement in the oxy-combustor. Hence the ASU will require high pressure air flow to cater to the higher oxygen demand. The low air compressor discharge pressure as indicated in Table 6 will be insufficient to feed air to the ASU.

A booster air compressor (as shown in Fig. 1) would thus be required to provide high pressure (10.5 bar in the design (BASE) case [40]) air to the ASU.

The gas turbine will be in part load operation in the retrofitted system. The thermal input to the GT combustor in the WAC design IGCC case with coal gasification [49] was 480.3 MW_{th}. Thermal inputs in the STEX case and SOFC-CC Retrofit STEX case are 347.2 MW_{th} and 267.9 MW_{th} respectively. It can thus be seen that the thermal input in these cases are about 73% and 56% of the design case respectively. With a 9% (on mass basis) syngas split stream fed to the SOFC, the mass flow rate at the gas turbine expander inlet reduces by 28% compared to the STEX case. The GT produces a power output of about 174 MW_e; a 27% reduction compared to the STEX case. Thus, the part load condition of the gas turbine when retrofitted with SOFCs and partial CO_2 capture is significant when compared with the STEX and design (BASE) IGCC case.

The GT part load condition and outlet temperature could be controlled to some extent using the variable inlet guide vanes (VIGV) [50]. It has been pointed out that until about 55–60% part load condition (based on GT thermal input/coupling power), the outlet temperature of the GT could be kept constant. In practice,

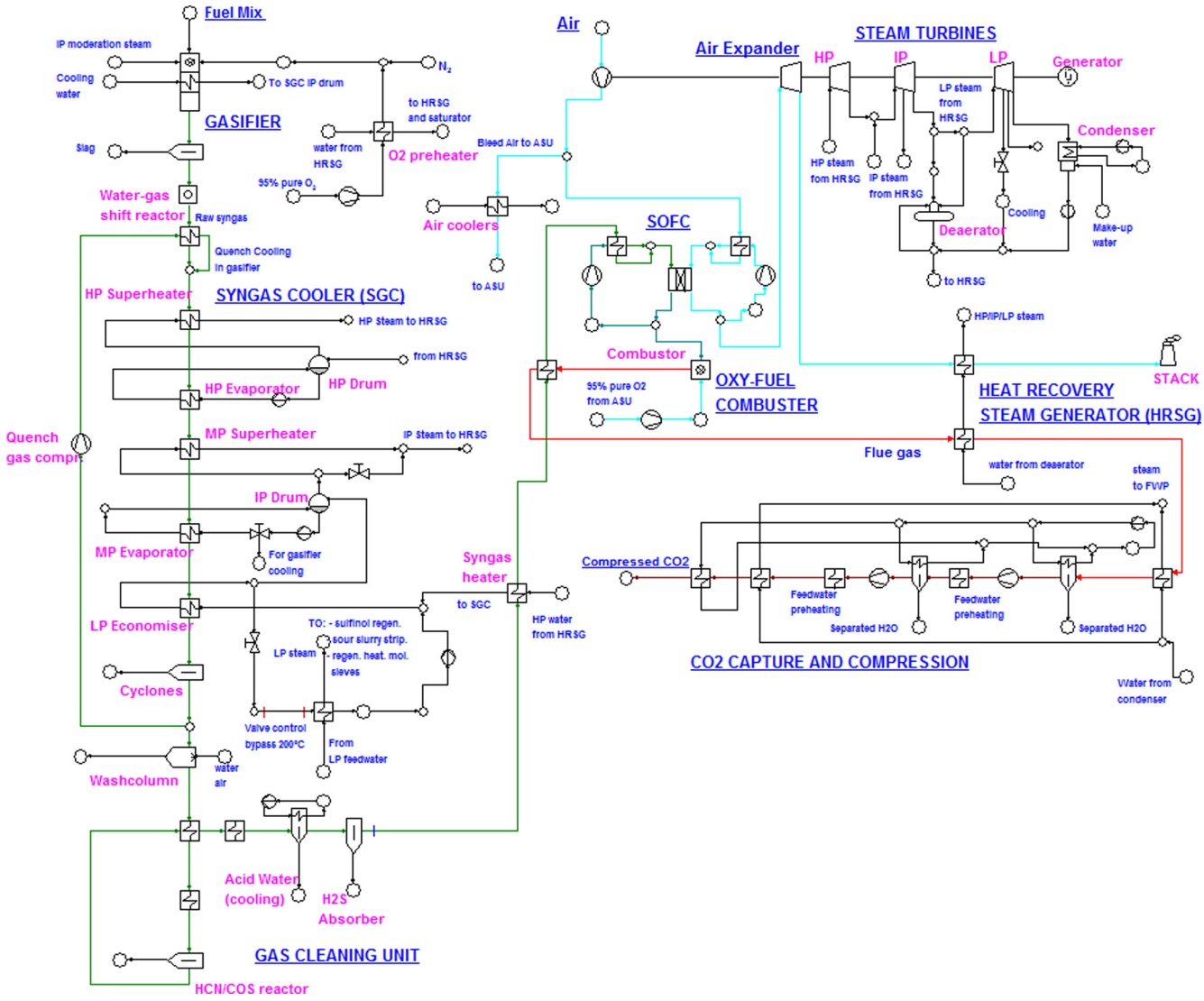

Fig. 4. Simplified process scheme for IGFC-CC STEX (full CO_2 capture) case – green streams represent syngas flow, red streams represent flue gas and blue streams represent air flow. Streams indicating detailed process/heat integration have been excluded to maintain clarity. (For interpretation of the references to colour in this figure legend, the reader is referred to the web version of this article.)

this is challenging because it is also necessary to maintain sufficient discharge pressure from the integrated air compressor for the ASU due to aforementioned reasons. The gas turbine will thus operate at a part load just within the range of the VIGVs. An important aspect to note is that with a small reduction in the GT outlet temperature, the inlet pressure will increase (Stodola's cone law) and consequently the SOFC pressure, voltage and power production will increase. Furthermore, the isentropic efficiency for the GT expander, air compressor and steam turbines has been assumed constant in this study. In reality, the isentropic efficiency of the GT will decrease when operating under part load [50]. However estimation of the isentropic efficiency under part load condition requires additional turbine data (performance maps) which is generally not readily available (often confidential information). For the steam turbines (particularly HP and IP turbine), a significant change in the isentropic efficiencies is not expected despite part load operation. The isentropic efficiency of these turbines (without governing stage) largely depend of the pressure ratio, volume flow and inlet temperature [51].

A syngas LHV range of about 4.3–5.5 MJ/kg is preferred for stable GT combustor operation at WAC. An important consideration with the SOFC-CC Retrofit STEX case is the 13% lower LHV of the syngas fuel to the combustor (see Table 7) compared to the STEX case. The difference in the clean syngas composition and LHV at the combustor inlet between both the cases arises due to the difference in N_2 dilution as aforementioned. In practice, a low (or high) LHV (<4.2 MJ/kg) lead to combustion/flame stability problems in the combustor as indicated by process engineers from the plant. This could lead to the need of a different combustor and/or fuel injectors [50,52]. This can be a major challenge as the GT burner might have to be suitably modified/replaced. Alternative methods of achieving a higher syngas LHV could be by adjusting syngas dilution and lower water vapour saturation, lower SOFC fuel utilization and lower syngas flow to SOFC (smaller SOFC stack). However all these measures would decrease the GT cycle and SOFC performance. Operation of the system with 70% torrefied woodpellets instead of 70% steam exploded woodpellets could also be a solution to increase LHV of the syngas fuel to the GT combustor. As the case presented here is a limiting case with maximum syngas split to the SOFC, the aforementioned alternative methods in principle should help achieve a higher syngas LHV when a smaller SOFC stack is used for retrofitting.

The SOFC stack in the retrofitted system produces a net power output of about 47.5 MW_e. An important thing to keep in mind is

Table 6
Model results SOFC-CC retrofit STEX – a comparison is presented with the STEX case.

	STEX (no CC)	SOFC-CC retrofit STEX (partial CC)		STEX (no CC)	SOFC-CC retrofit STEX (partial CC)
Fuel Input			HP Turbine inlet temperature, °C	473.71	516.04
Input pulverized fuel, kg/s	23.74	23.74	HP Turbine Outlet temperature, °C	311.92	346.22
LHV, MJ/kg	19.59	19.59	HP Steam mass flow, kg/s	65.64	62.04
Thermal input, MW_{th}	465.00	465.00	IP Steam turbine inlet pressure, bar	23.82	23.25
Gasifier			IP Steam turbine outlet pressure, bar	3.59	3.37
Outlet pressure, bar	24.90	24.90	IP Turbine inlet temperature, °C	463.50	499.65
Outlet temperature, °C	1515.00	1515.00	IP Turbine Outlet temperature, °C	227.34	250.00
Oxygen mass flow, kg/s	14.74	14.74	IP Steam mass flow, kg/s	80.13	76.55
Moderation steam, kg/s	1.18	1.18	LP Steam turbine inlet pressure, bar	3.59	3.34
Quench gas recycle, kg/s	52.42	52.42	*SOFC unit*		
Temperature quench gas, °C	243.40	243.17	Fuel LHV, MJ/kg	–	10.42
Quench pressure after compres.,bar	24.90	24.90	Anode flow (in), kg/s	–	18.45
Syngas cooler			Anode flow (out), kg/s	–	23.17
Syngas inlet temperature, °C	820.00	820.00	Anode recirculation flow, kg/s	–	9.44
Syngas outlet temperature, °C	229.40	229.17	Cathode flow (in), kg/s	–	252.69
HP steam to HRSG, kg/s	36.82	35.02	Cathode flow (out), kg/s	–	247.97
HP steam to HRSG: Temperature, °C	363.90	367.09	Cathode recirculation flow, kg/s	–	81.60
IP steam to HRSG, kg/s	15.60	16.15	Voltage, V	–	0.83
IP steam to HRSG: Temperature, °C	321.69	318.14	Active Area, m^2	–	22785.97
LP steam: Pressure, bar	9.00	9.00	Anode recir. compressor consumption, kW_e	–	39.70
LP steam: Temperature, °C	175.36	175.36	Cathode recir. compressor consumption, kW_e	–	372.53
LP steam: Mass flow, kg/s	4.34	4.31	**Power**, MW_e	–	**47.55**
Cyclone			*Oxy-fuel CC*		
Outlet temperature syngas, °C	229.39	229.17	CO_2 purity, mol%	–	89.09
Wash column			Captured CO_2 flow, kg/s	–	11.69
Outlet mass flow syngas, kg/s	40.93	40.94	Oxygen flow to oxy-combustor, kg/s	–	0.93
Pressure syngas, bar	24.52	24.52	Oxy-combustor temperature, °C	–	1567.28
Outlet temperature syngas, °C	145.10	146.36	Oxy-combustor pressure, bar	–	7.00
HCN/COS reactor			CO_2 compressor 1 outlet pressure, bar	–	32.25
Outlet temperature syngas, °C	191.80	192.00	CO_2 compressor 2 outlet pressure, bar	–	152.26
Outlet pressure, bar	21.72	21.72	Cooling water flow, kg/s	–	193.15
H_2S absorber			CO_2 compressor 1 consumption, MW_e	–	1.83
Outlet temperature syngas, °C	40.00	40.00	CO_2 compressor 2 consumption, MW_e	–	1.48
Mass flow syngas, kg/s	33.14	33.14	Condensed water flow, kg/s	–	1.98
Gas preparation			Generated steam flow, kg/s	–	3.05
Nitrogen temperature, °C	59.00	59.00	*HRSG*		
Nitrogen pressure, bar	12.01	12.01	HP Steam raising mass flow, kg/s	28.80	27.02
Nitrogen mass flow, kg/s	38.00	33.00	HP Superheater outlet temperature, °C	476.34	516.04
Saturator syngas outlet temperature, °C	119.62	125.00	HP Superheater outlet pressure, bar	97.93	96.06
Preheater syngas outlet temperature, °C	292.41	283.56	LP Steam raising mass flow, kg/s	4.15	1.71
Powerblock			LP Superheater outlet temperature, °C	233.25	269.99
Air compressor discharge, bar	9.05	7.42	LP Superheater outlet pressure, bar	3.59	2.77
Air bleed, kg/s	61.90	72.63	*Power output*		
Combustion chamber pressure, bar	8.78	7.24	Gross Power output, MW_e	204.85	223.64
Gas Turbine inlet temperature, °C	919.20	950.00	Auxiliary load, MW_e	31.82	34.04
HP Steam turbine inlet pressure, bar	92.93	96.06	**Net Power output**, MW_e	**173.02**	**189.59**
HP Steam turbine outlet pressure, bar	27.82	27.25	**Net efficiency**, %	**37.20**	**40.77**

Table 7
Clean syngas composition (mol%), input to GT combustor.

Case	H_2	N_2	AR	CH_4	CO	CO_2	H_2O	H_2S	LHV, MJ/kg
STEX	11.89	43.00	0.37	0.00	25.99	3.00	15.75	0.00	**4.28**
SOFC-CC Retrofit STEX	10.32	44.07	0.32	0.00	22.58	2.61	20.10	0.00	**3.73**

that this is for a thermodynamically limiting case; where we try to show the real thermodynamic/process constraints with existing plant equipment. The study clearly indicates that smaller stacks (with power levels from kW_e to 40 MW_e) can be integrated in existing IGCC power plants without major thermodynamic/process implications. Most power utility companies and organizations are currently focussing towards large scale newly designed IGFC power plants. The authors believe that an alternative and more logical approach towards introducing SOFCs in IGCC power plants is to carry out a step wise integration (retrofitting). The size of the SOFC stack should be incremented gradually, synchronous with latest technology development. Commercial syngas fed SOFC modules are currently available [37,38] in the kW_e to 1 MW_e range and such units should be considered to retrofit in existing IGCC plants. Step wise scaling up in the size of the SOFC stack module will also promote technology development to some extent, as operating/practical challenges with real syngas can be identified even while operating with smaller SOFC stacks.

Table 8 shows the model results for the IGFC-CC STEX case with a comparison to the STEX case. The net electrical efficiency of 47.9% is comparable with values reported in literature for coal based IGFC-CC systems [19,14,22]. Absence of N_2 dilution leads to the absence of ASU N_2 compression, which is a major contributor in the auxilliary load (refer to our previous article [12]). Process parameters upstream gas preparation are very comparable between both the cases. Notable differences are a higher IP, LP

Table 8
Model results IGFC-CC STEX – a comparison is presented with the STEX case.

	STEX (no CC)	IGFC-CC STEX (full CC)		STEX (no CC)	IGFC-CC STEX (full CC)
Fuel Input			HP Turbine inlet temperature,°C	473.71	507.72
Input pulverized Coal, kg/s	23.74	23.74	HP Turbine Outlet temperature,°C	311.92	322.29
LHV, MJ/kg	19.59	19.59	HP Steam mass flow, kg/s	65.64	46.64
Thermal input, MW_{th}	465.00	465.00	IP Steam turbine inlet pressure, bar	23.82	29.00
Gasifier			IP Steam turbine outlet pressure, bar	3.59	4.25
Outlet pressure, bar	24.90	24.90	IP Turbine inlet temperature, °C	463.50	510.00
Outlet temperature, °C	1515.00	1515.00	IP Turbine Outlet temperature, °C	227.34	256.76
Oxygen mass flow, kg/s	14.74	14.73	IP Steam mass flow, kg/s	80.13	61.23
Moderation steam, kg/s	1.18	1.18	LP Steam turbine inlet pressure, bar	3.59	4.25
Quench gas recycle, kg/s	52.42	52.70	*SOFC unit*		
Temperature quench gas, °C	243.40	246.95	Fuel LHV, MJ/kg	–	10.43
Quench pressure after compres.,bar	24.90	24.90	Anode flow (in), kg/s	–	68.19
Syngas cooler			Anode flow (out), kg/s	–	85.60
Syngas inlet temperature, °C	820.00	820.00	Anode recirculation flow, kg/s	–	35.05
Syngas outlet temperature, °C	229.40	232.85	Cathode flow (in), kg/s	–	917.13
HP steam to HRSG, kg/s	36.82	33.77	Cathode flow (out), kg/s	–	899.71
HP steam to HRSG: Temperature, °C	363.90	373.17	Cathode recirculation flow, kg/s	–	760.90
IP steam to HRSG, kg/s	15.60	16.23	Voltage, V	–	0.83
IP steam to HRSG: Temperature, °C	321.69	326.97	Active Area, m^2	–	84015.12
LP steam: Pressure, bar	9.00	9.00	Anode recir. compressor consumption, $kW_{it\ e}$	–	96.82
LP steam: Temperature, °C	175.36	175.36	Cathode recir.compressor consumption, kW_e	–	2408.60
LP steam: Mass flow, kg/s	4.34	5.02	**Power**, MW_e	–	**167.61**
Cyclones			*Oxy-fuel CC*		
Outlet temperature syngas, °C	229.39	232.85	CO_2 purity, mol%	–	89.12
Wash column			Captured CO_2 flow, kg/s	–	43.09
Outlet mass flow syngas, kg/s	40.93	40.99	Oxygen flow to oxy-combustor, kg/s	–	3.41
Pressure syngas, bar	24.52	24.52	Oxy-combustor temperature, °C	–	1567.62
Outlet temperature syngas, °C	145.10	146.69	Oxy-combustor pressure, bar	–	10.15
HCN/COS reactor			CO_2 compressor 1 outlet pressure,bar	–	41.08
Outlet temperature syngas, °C	191.80	192.00	CO_2 compressor 2 outlet pressure, bar	–	150.80
Outlet pressure, bar	21.72	21.72	Cooling water flow, kg/s	–	1299.13
H_2S absorber			CO_2 compressor 1 consumption,MW	–	6.10
Outlet temperature syngas, °C	40.00	40.00	CO_2 compressor 2 consumption, MW	–	4.14
Mass flow syngas, kg/s	33.14	33.14	Condensed water flow, kg/s	–	7.32
Gas preparation			Generated steam flow, kg/s	–	6.89
Nitrogen temperature, °C	59.00	–	*HRSG*		
Nitrogen pressure, bar	13.01	–	HP Steam raising mass flow, kg/s	28.80	12.87
Nitrogen mass flow, kg/s	38.00	–	HP Superheater outlet temperature, °C	476.34	507.72
Saturator syngas outlet temperature, °C	119.62	–	HP Superheater outlet pressure, bar	97.93	119.80
Preheater syngas outlet temperature, °C	292.41	270.00	LP Steam raising mass flow, kg/s	4.15	12.87
Powerblock			LP Superheater outlet temperature, °C	233.25	255.00
Air compressor discharge, bar	9.05	10.50	LP Superheater outlet pressure, bar	3.59	4.25
Air bleed, kg/s	61.90	86.43	*Power output*		
Combustion chamber pressure, bar	8.78	–	Gross Power output, MW_e	204.85	260.49
Gas Turbine/Air expander inlet temperature, °C	919.20	950.00	Auxiliary load, MW_e	31.82	37.44
HP Steam turbine inlet pressure, bar	92.93	119.80	**Net Power output**, MW_e	**173.02**	**223.05**
HP Steam turbine outlet pressure, bar	27.82	32.70	**Net efficiency**, %	**37.20**	**47.96**

steam flow in the SGC and a lower syngas temperature after preheating. The increase in the IP/LP steam production in the SGC is particularly due to a marginally higher (0.3%) syngas flow (the temperatures are very similar).

Considering that the SOFC is the main power producing unit in the IGFC-CC STEX case, significant differences can be observed between both systems in the power block and HRSG. Despite the same amount of clean syngas used to generate power in the SOFC stack, there is a considerable reduction (about 55% on mass basis) in the HRSG HP steam production. The LP steam production is however about 3 times higher.

This is due to the complex design of SOFC module (anode/cathode recirculation) and HRSG, where two heat sources, namely the expanded air and CO_2 rich flue gas are utilized. However the net power produced by the steam turbines (HP/IP/LP) is only about 9% lower than the STEX case. The important point to note is that oxy-combustion CO_2 capture has a relatively large negative effect on the net plant efficiency. The auxilliary load in the IGFC-CC STEX case is about 5.6 MW (19%) higher than the STEX case mainly due to the 2 stage CO_2 compression in the CO_2 capture unit. Air bleed for the ASU from the air compressor is also increased due to additional oxygen requirements in the oxy-fuel combustor which leads to an increase in the auxilliary load due to additional O_2 compression. However due to the absence of the dilution N_2 compressor and reduced power consumption in the HP water pump, the increase in auxilliary load is not drastic. As seen from Table 8, the stored CO_2 stream is about 89% pure. The gas mixture consists of about 9% N_2, 1.5% of Ar and trace quantities of O_2 and H_2O. Presence of O_2 is due to the slight oxygen excess in the oxy-fuel combustor ($\lambda = 1.05$). Argon and a part of N_2 originate from the 95% pure O_2 mixture from the ASU used in the gasifier and oxy-fuel combustor. The remaining N_2 comes from the fuel and the fuel transport gas to the gasifier.

The SOFC unit produces a net power of about 157 MW_e which is about 73% of the net plant power output. The anode and cathode recirculation compressor power consumptions are much higher

Table 9
Anode outlet gas composition (mol%), input to oxy-fuel combustor.

Case	H_2	N_2	AR	CH_4	CO	CO_2	H_2O	H_2S	LHV, MJ/kg
SOFC-CC Retrofit STEX	3.25	6.40	0.84	0.00	9.58	55.94	23.98	0.00	**1.03**
IGFC-CC STEX	3.26	6.39	0.84	0.00	9.59	57.91	24.01	0.00	**1.03**

compared to the SOFC-CC Retrofit STEX case due to the higher gas flow rates. Table 9 shows the anode outlet gas compositions and LHV from the SOFC unit for both the cases:

The LHV of the outlet gas is considerably low and it is assumed that the oxy-fuel combustor (newly designed) can cope with this. In case of unstable operation, however pure syngas could be partly utilized. In the IGFC-CC STEX case, it is important to note that the low LHV fuel to the oxy-fuel combustor leads to low thermal input to the air expander. This leads to a lower thermal energy in the HRSG and consequently lower power production from the steam turbines.

4.1. Carbon deposition

Operating SOFCs with syngas as fuel certainly offers advantages in terms of boosting efficiencies and flexibility. However, an important operating challenge is to prevent carbon deposition/coking. Under certain operating conditions, syngas and CO decompose to create solid carbon formations in Ni-based anodes or anode inlet/outlet pipes [53,54]. The electrochemical performance of the anode then drastically reduces due to a decrease in the active area, which also results in a large polarization resistance. The SOFC model in this study has been developed under the assumption of an Ni-GDC anode (Table 4) and hence it is important to assess the possibility of carbon deposition. Ternary phase diagrams based on thermochemical equilibrium calculations (free energy minimization) are useful to predict the theoretical boundary limits for carbon deposition depending on the operating condition [55].

In order to assess the possibilities of carbon deposition in both the cases, operating conditions have been considered at three locations within the system as listed in Table 10. Based on these conditions, equilibrium calculations have been performed using the software Factsage [56] to obtain the C-H-O ternary phase diagram (Fig. 5). Fig. 5a and b are the ternary phase diagrams for the SOFC-CC Retrofit STEX and IGFC-CC STEX case respectively. The red[1] curve represents the boundary limits for the gas conditions at the anode inlet before recirculation and point A represents the actual operating point. The green curve represents the boundary limits for the gas conditions at the anode inlet after recirculation and point B represents the actual operating point. The blue curve represents the boundary limits for the gas conditions at the anode outlet after recirculation and point C represents the actual operating point.

As seen from both the figures, point A lies above the corresponding equilibrium curve indicating a possibility of coking. The conditions at the actual inlet to the SOFC anode (point B) and the anode outlet (point C) are below the corresponding equilibrium curves thus indicating theoretically safe operating conditions. Addition of steam to the extracted syngas is a possible option to reduce the possibility of coking at point A [54]. However it is important to note that steam should then be extracted from the system and this will lead to drop in the net electrical efficiency. Preliminary calculations for the SOFC-CC Retrofit STEX case indicate that the drop in net electrical efficiency could be about 0.2–0.5% points with IP steam extraction from the syngas cooler. Considering the scope of the article, a detailed analysis on this has not been presented in this article. Carbon deposition also depends on other factors like residence time, reaction/surface conditions in pipes etc. Despite possibilities of carbon deposition in the SOFC upstream sections (pipes) of the system i,e from the GCU to the SOFC unit or after the syngas cooler, process engineers at WAC have not observed any significant coking in the past in these lines during normal operation with coal or biomass. Hence it is assumed that the operating conditions upstream the syngas preheaters and SOFC unit are safe to prevent carbon deposition. This article indicates the risks of carbon deposition (particularly in the SOFC inlet), however additional investigations regarding carbon deposition in SOFC retrofitted IGCC systems is highly encouraged.

[1] For interpretation of colour in Fig. 5, the reader is referred to the web version of this article.

Table 10
Operating points/locations considered to evaluate the systems for carbon deposition.

Point	Location	Pressure, bar (SOFC-CC Retrofit STEX/IGFC-CC STEX)	Temperature, °C
A	Anode inlet (pipe) before recirculation	7.35/10.50	750.00
B	Anode inlet (pipe) after recirculation	7.32/10.48	850.00
C	Anode outlet (pipe)	7.27/10.43	950.00

4.2. Exergy analysis

Exergy analysis is an important tool in thermodynamic system evaluation as it helps to identify locations and true magnitudes of loss [57]. Cycle-Tempo offers a possibility to carry out an exergy analysis (2nd law analysis). The exergy of matter is calculated as the reversible (maximum) work derived by bringing matter in thermomechanical and chemical equilibrium with the reference environment. Thus the exergy of matter is calculated as a sum of the thermomechanical and chemical exergies. In principle, the kinetic and potential exergies are also included but since they do not usually change significantly, this is neglected in the calculation. In order to quantify the exergy loss/destruction; the exergy of matter, exergy of heat (in case of heat transfer to/from the environment) and exergy of work (in case of work generation/consumption) is calculated for all streams/components [58]. The exergy loss/destruction is then calculated as the difference between the incoming and outgoing exergy. Exergy destruction is associated with the internal irreversibilities (entropy generation) while exergy loss is associated with the transfer of exergy (through material and energy streams) to the environment [59].

In principle, exergy efficiency is calculated for each component by the program with appropriate product and source(s) consideration. Detailed information on this can be found in the program manual [60,58]. The total exergy efficiency (η_{ex}) for the system is calculated according to Eq. (10), where Ex_{source}, $Ex_{product}$ and Ex_{loss} represent the source exergy (exergy of fuel), product exergy (net power) and total exergy loss (includes the total exergy destruction) respectively:

$$\eta_{ex} = \frac{Ex_{product}}{Ex_{source}} = \frac{Ex_{source} - Ex_{loss}}{Ex_{source}} \quad (10)$$

The exergy of the solid fuel mix (Exergy input) is estimated by Cycle Tempo using a method described by Baehr [61]. Table 11 gives an overview of energy (1st law) and exergy (2nd law)

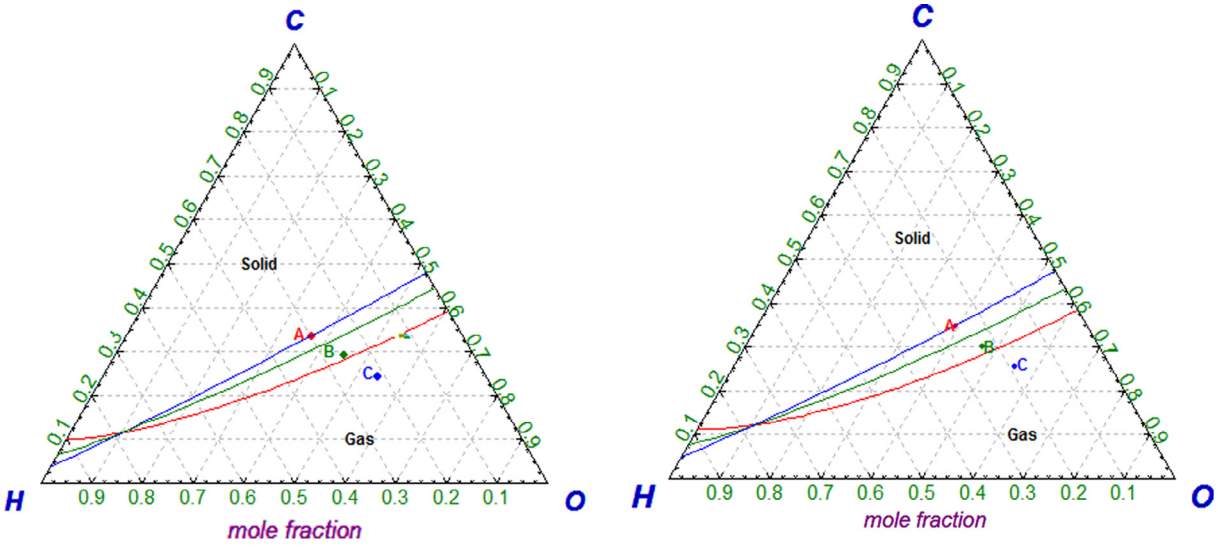

Fig. 5. Ternary phase diagram showing equilibrium lines and operating points to indicate possibilities of carbon deposition.

Table 11
Exergy output and exergy efficiency for various cases.

	STEX		SOFC-CC Retrofit STEX		IGFC-CC STEX	
	Energy	Exergy	Energy	Exergy	Energy	Exergy
Input, MW	465.06	510.50	465.06	510.50	465.06	510.50
Gross Power, MW	204.85	204.85	223.64	223.64	260.50	260.50
Auxilliary load, MW	31.82	31.82	34.04	34.04	37.44	37.44
Net Power, MW	173.02	173.02	189.59	189.59	223.05	223.05
Net efficiency, %	**37.20**	**33.89**	**40.77**	**37.13**	**47.96**	**43.68**

analysis for the 2 cases in comparison with the STEX case. An exergy efficiency of about 37% is obtained with the retrofitted system indicating that existing IGCC plants can still be operated with higher electrical/exergy efficiencies (about 12% higher) with retrofitting direct internal reforming solid oxide fuel cells and oxy-fuel CO_2 capture technologies. This efficiency boost with a relatively low carbon footprint can be considered as a possible solution to operate existing power plants with reduced emissions and high efficiency in near future. With a newly designed IGFC power plant with oxy-combustion CO_2 capture, a much higher exergy efficiency of about 44% is obtained. The increase in the exergy efficiency due to electrochemical fuel conversion is compensated with exergy losses and exergy destruction in the CO_2 capture unit. However, there is an increase of about 10 percentage points (25% increase) in the exergy efficiency.

Fig. 6 shows the exergy flow diagram for the SOFC-CC Retrofit STEX case illustrating the exergy loss/destruction due to various operations in the plant. Exergy loss and destruction due to the partial CO_2 capture account for about 1.2% of the total exergy losses. In comparison with the STEX case [12], the stack losses are also lower due to the lower concentrations of CO_2 and H_2O. The SOFC system including the SOFC stack contributes to a relatively low extent (3.5%) in the total exergy losses. Exergy destruction during gasification and combustion still contribute largely to the irreversibilities in the system, however an important observation to be noted is the reduced exergy destruction in the GT combustor. The exergy destruction in the GT combustor in the STEX case is about 97.6 MW; about 19% of the total exergy losses [12]. The partial replacement of fuel combustion with electrochemical conversion leads to a 30% reduction in the exergy destruction in the GT combustor. Hence despite the utilization of oxy-combustion CO_2 capture, it is seen that retrofitting SOFCs in existing IGCC power plants is beneficial from the exergy/electrical efficiency point of view.

Fig. 7 shows the exergy flow diagram for the IGFC-CC STEX case. The CO_2 capture unit contributes with about 8% to the total exergy losses. As it can be seen, gasification is the largest source of exergy destruction. Complete replacement of combustion with electrochemical oxidation in the SOFC unit leads to a reduction in total exergy losses with exergy destruction in the SOFC unit being relatively low (<5%). Exergy loss through the exhaust stack (air) is largely negligible. The figure shows a combined loss/destruction of about 3.5% in the gas cleaning unit and due to syngas preheating.

From the exergy analysis of both systems it can be seen that retrofitting IGCC plants with SOFC-CO_2 capture offers significant thermodynamic advantages in terms of boosting electrical and exergy efficiencies. Despite concerns regarding material, cost and scaling up; further research (particularly market based and thermo-economic evaluations) of solid oxide fuel cell integration in existing large scale bio-IGCC power plants is highly encouraged.

4.3. CO_2 neutrality and emissions

Power production with high percentage of biomass in the fuel blend offers a possibility to design a CO_2 neutral/negative system. Estimation of biomass CO_2 neutrality is generally based on an assumption that biomass removes as much CO_2 from the environment during its growth as is released during its combustion. This work like majority literature articles assumes the wood pellet biomass as a CO_2 neutral fuel. Table 12 shows a parametric

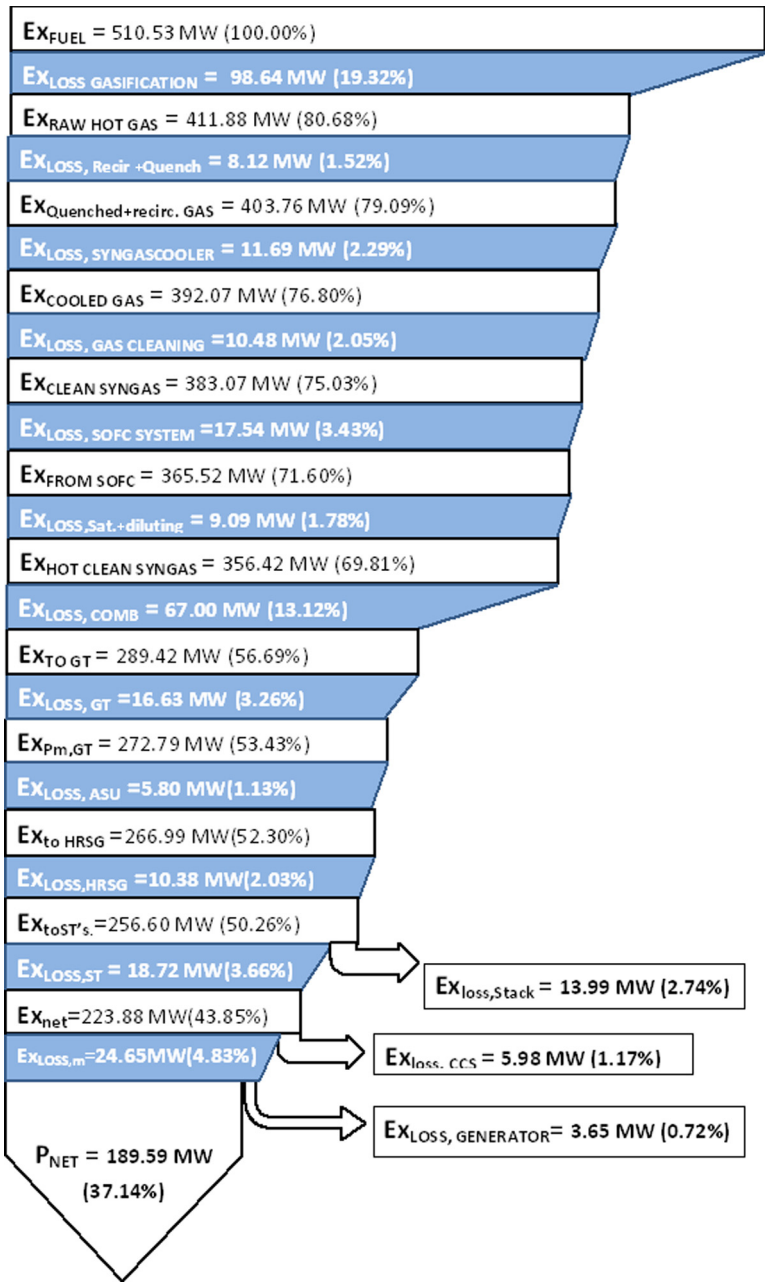

Fig. 6. Exergy flow diagram for SOFC-CC Retrofit STEX (with partial CC) case – exergy destruction during GT combustion are lower than the STEX case with the partial replacement of combustion with electrochemical oxidation in the SOFC.

comparison between the various cases considering CO_2 neutrality and emissions. The fuel input in all the three cases is a blend of 70% biomass and 30% coal (energy based). Based on our assumption, this means that even without CO_2 capture (STEX case), the system is 70% CO_2 neutral. The remaining undesired CO_2 emission originates from the 30% coal in the fuel blend.

In order to estimate CO_2 neutrality, the total CO_2 flow in the system has first been calculated as the sum of CO_2 co-absorbed in the H_2S absorber [12], CO_2 released through the stack and the pure captured CO_2 in the CO_2 capture unit. The CO_2 co-absorbed in the H_2S absorber is part of emissions as this is just vented out from the plant. The net emitted CO_2 from the system is a sum of the vented CO_2 from the H_2S absorber and the CO_2 released through the stack. The pure captured CO_2 has been calculated based on the purity of the CO_2 stream (Tables 6 and 7). With a fixed fuel input mass flow, the amount of CO_2 produced per unit mass of fuel (fuel specific CO_2, γ) is calculated. The fuel specific CO_2 from pure coal (γ_{coal}) has been calculated to be 2.45 based on the BASE (with no biomass co-gasification) case (The BASE case has been described in detail in our previous article [49]). As the STEX blend contains less carbon and more oxygen than coal [12], the fuel specific CO_2 is much lower than with pure coal. The coal based CO_2 flow is then calculated as shown in Eq. (11):

$$\text{Coal based } CO_2 = 0.3 \cdot \text{Fuel input} \cdot \gamma_{coal} \tag{11}$$

The coal based CO_2 capture fraction is then calculated with Eq. (12):

$$\text{Coal based } CO_2 \text{ capture fraction} = \frac{\text{Captured } CO_2}{\text{Coal based } CO_2} \tag{12}$$

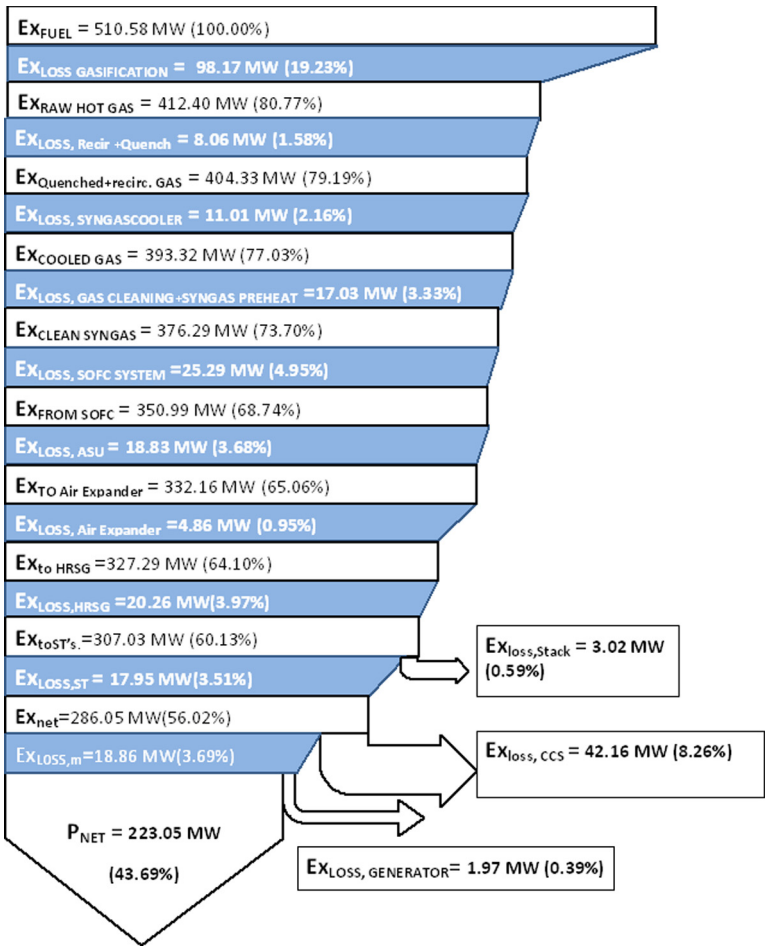

Fig. 7. Exergy flow diagram for IGFC-CC STEX (full CC) case – high exergy loss/destruction due to CO_2 capture is compensated by the high efficiency SOFC system rendering a relatively high net exergy efficiency.

Table 12
System evaluation for CO_2 neutrality and emissions.

Parameter	STEX (no CC)	SOFC-CC retrofit STEX (partial CC)	IGFC-CC STEX (full CC)
Fuel Input, kg/s	23.74	23.74	23.74
Co-absorbed CO_2 in H_2S absorber, kg/s	1.89	1.91	1.90
CO_2 in stack (exhaust), kg/s	43.25	31.53	0.06
Captured CO_2, kg/s	**0**	**11.70**	**43.09**
Total CO_2, kg/s	45.14	45.14	45.07
Fuel specific CO_2 (γ), kg CO_2/kg_{fuel}	1.90	1.90	1.89
Coal based CO_2, kg/s	17.48	17.48	17.48
Coal based CO_2 capture fraction, %	0	0.67	2.46
CO_2 neutrality factor,	**0.70**	**0.90**	**1.44**
CO_2 emitted, kg/s	45.14	33.44	1.98
Net Power Output, MW_e	173.02	189.59	223.05
Specific CO_2 emitted, kg/kW h_e	**0.93**	**0.64**	**0.03**

In order to assess the amount of CO_2 emitted per unit power produced, the specific CO_2 emitted (ratio of CO_2 emitted and net power output) has also been calculated and shown in Table 12. The CO_2 neutrality factor then has been calculated based on Eq. (13):

$$CO_2 \text{ neutrality factor} = 0.7 + 0.3.(\text{Coal based } CO_2 \text{ capture fraction}) \quad (13)$$

Applying full CO_2 capture to 70% biomass co-gasified IGCC power plants results in a CO_2 neutrality of higher than 100%, or a CO_2 negative system. As it can be seen from Table 12 the SOFC-CC Retrofit STEX system is 90% CO_2 neutral while the IGFC-CC system is 43% CO_2 negative. The specific CO_2 emitted for the STEX case are comparable to values cited in literature for biomass co-gasification [62,63]. Retrofitting with CO_2 capture (SOFC-CC Retrofit STEX case) reduces the specific emissions by almost 45% and application of full scale CO_2 capture (IGFC-CC STEX case) leads to a very low specific CO_2 emission.

Feasibility and sensitivity studies towards sizing the SOFC stack module and CO_2 capture unit for retrofitting is highly recommended. It has been indicated in this article that coking/carbon deposition is a major risk (particularly at the SOFC anode inlet pipes) in the retrofitted system. Detailed investigations on this aspect giving possible solutions are highly recommended as future work. SOFC operation with real syngas also needs experimental and system investigation. In addition, the gas turbine part load operation and ways to minimize its effect on the plant performance should be further researched upon.

5. Conclusions

The article presents, for the first time, a case study towards introducing (retrofitting) solid oxide fuel cells (SOFCs) and CO_2 capture in existing IGCC power plants utilizing high percentage (up to 70%) biomass co-gasification with a focus on near future

implementation. The approach and conclusions are equally applicable for coal based IGCC power plant systems. Various thermodynamic aspects have been addressed and process modifications have been identified to retrofit SOFCs in IGCC systems. The main conclusions of the study are listed below:

- Existing integrated gasification combined cycle power plants (coal/biomass based) could be operated without major plant modifications and relatively high electrical efficiencies of more than 40%(LHV) by retrofitting with solid oxide fuel cells (SOFC) (producing up to 40 MW_e electric power) and partial oxy-combustion CO_2 capture.
- Control of the GT expander outlet temperature with variable inlet guide vanes (VIGV) to minimize part load effects is crucial when retrofitted with SOFCs.
- The discharge pressure from the main air compressor is much lower (about 18%) in the retrofitted system. In order to meet the oxygen demand and to feed bleed air to the ASU at design pressure, a booster air compressor would be required.
- Resizing the SOFC stack and/or modifications in the N_2 dilution and water saturation unit might be required to obtain an acceptable LHV for clean syngas; thus enduring flame stability in the GT combustor.
- Retrofitting with SOFC and partial oxy-combustion CO_2 capture leads to a considerable (about 12% in our limiting case) reduction in the IP/LP steam production due to the lower syngas flow (and hence heat transfer) in the combined cycle.
- To apply full scale integration of SOFC and oxy-combustion CO_2 capture (IGFC-CC STEX case), the flue gas GT expander should be replaced by an air expander and the WAC design based HRSG has to be significantly redesigned.
- Exergy (2nd law) analysis indicates that exergy destruction due to GT combustion reduce significantly (about 30%) in the retrofitted system due to partial replacement with electrochemical conversion. Total exergy efficiency increases to about 37% (increase by 9%) when retrofitted with SOFC and partial oxy-combustion CO_2 capture.
- CO_2 negative IGFC power plants can be developed by utilizing 70% biomass in the fuel feed and full oxy-combustion CO_2 capture. Retrofitting with partial CO_2 capture reduces the specific emissions by almost 45% and application of full scale CO_2 capture leads to a very low specific CO_2 emission.

Based on the process constraints presented in this article, appropriate engineering solutions should be developed by the industry. Despite concerns on costs and scaling up issues, model based thermodynamic evaluations as presented in this article are very important to assess plant performance with alternative and safe operating conditions. In addition, the thermodynamic analysis and results presented in this article are helpful to further evaluate design/sizing challenges in SOFC-CO_2 capture retrofitted IGCC power plant systems for near future implementation, gas turbine part load behaviour and techno-economic aspects.

Acknowledgements

The research was partly supported by funding from the CATO-2B project, the Dutch national project on carbon capture and storage (CCS).

References

[1] United Nations Framework Convention on Climate Change (UNFCCC), Report of the Conference of the Parties on its twenty-first session, held in Paris from 30 November to 13 December 2015, January 2016. <http://unfccc.int/resource/docs/2015/cop21/eng/10.pdf>.

[2] European Climate Foundation, ROADMAP 2050 A practical guide to a properous low-carbon Europe - Technical Analysis, Tech. rep., European Commission, 2010. <http://www.roadmap2050.eu/attachments/files/Volume1_fullreport_PressPack.pdf>.

[3] European Commission, A policy framework for climate and energy in the period from 2020 to 2030, Tech. rep., European Commission, 2014. <http://eur-lex.europa.eu/legal-content/EN/TXT/PDF/?uri=CELEX:52014DC0015&from=EN>.

[4] E. Commision, Analysis of options to move beyond 20 assessing the risk of carbon leakage, Tech. rep., E U commision/EUparliament, 2010. <http://eur-lex.europa.eu/legal-content/EN/TXT/PDF/?uri=CELEX:52010DC0265&from=EN>.

[5] D.L. Sanchez, J.H. Nelson, J. Johnston, A. Mileva, D.M. Kammen, Biomass enables the transition to a carbon-negative power system across western north america, Nat. Clim. Change 5 (3) (2015) 230–234, http://dx.doi.org/10.1038/nclimate2488.

[6] D.L. Sanchez, D.M. Kammen, A commercialization strategy for carbon-negative energy, Nat. Energy 1 (2016) 15002, http://dx.doi.org/10.1038/nenergy.2015.2.

[7] J.S. Rhodes, D.W. Keith, Engineering economic analysis of biomass IGCC with carbon capture and storage, Biomass Bioenergy 29 (6) (2005) 440–450, http://dx.doi.org/10.1016/j.biombioe.2005.06.007. <http://www.sciencedirect.com/science/article/pii/S096195340500098X>.

[8] D. Klein, N. Bauer, B. Bodirsky, J.P. Dietrich, A. Popp, Bio-igcc with CCS as a long-term mitigation option in a coupled energy-system and land-use model, Energy Procedia 4 (2011) 2933–2940, http://dx.doi.org/10.1016/j.egypro.2011.02.201, 10th International Conference on Greenhouse Gas Control Technologies <http://www.sciencedirect.com/science/article/pii/S1876610211003985>.

[9] C. Kunze, H. Spliethoff, Assessment of oxy-fuel, pre- and post-combustion-based carbon capture for future IGCC plants, Appl. Energy 94 (2012) 109–116, http://dx.doi.org/10.1016/j.apenergy.2012.01.013. <http://www.sciencedirect.com/science/article/pii/S0306261912000190>.

[10] M. Kanniche, R. Gros-Bonnivard, P. Jaud, J. Valle-Marcos, J.-M. Amann, C. Bouallou, Pre-combustion, post-combustion and oxy-combustion in thermal power plant for CO2 capture, Appl. Therm. Eng. 30 (1) (2010) 53–62, http://dx.doi.org/10.1016/j.applthermaleng.2009.05.005, selected Papers from the 11th Conference on Process Integration, Modelling and Optimisation for Energy Saving and Pollution Reduction <http://www.sciencedirect.com/science/article/pii/S1359431109001471>.

[11] N. Woudstra, T.P. van der Stelt, K. Hemmes, The thermodynamic evaluation and optimization of fuel cell systems, J. Fuel Cell Sci. Technol. 3 (2) (2006) 155–164, http://dx.doi.org/10.1115/1.2174064.

[12] A. Thallam Thattai, V. Oldenbroek, L. Schoenmakers, T. Woudstra, P.V. Aravind, Experimental model validation and thermodynamic assessment on high percentage (up to 70 biomass co-gasification at the 253 MWe integrated gasification combined cycle power plant in Buggenum, The Netherlands, Appl. Energy 168 (2016) 381–393, http://dx.doi.org/10.1016/j.apenergy.2016.01.131. <http://www.sciencedirect.com/science/article/pii/S0306261916301192>.

[13] H. Spliethoff, Power generation from solid fuels, Coal-Fuelled Combined Cycle Power Plants, Springer Berlin Heidelberg, Berlin, Heidelberg, 2010, pp. 469–628, http://dx.doi.org/10.1007/978-3-642-02856-4_7, ch..

[14] S.K. Park, T.S. Kim, J.L. Sohn, Y.D. Lee, An integrated power generation system combining solid oxide fuel cell and oxy-fuel combustion for high performance and CO_2 capture, Appl. Energy 88 (4) (2011) 1187–1196, http://dx.doi.org/10.1016/j.apenergy.2010.10.037. <http://www.sciencedirect.com/science/article/pii/S0306261910004393>.

[15] S.K. Park, J.-H. Ahn, T.S. Kim, Performance evaluation of integrated gasification solid oxide fuel cell/gas turbine systems including carbon dioxide capture, Appl. Energy 88 (9) (2011) 2976–2987, http://dx.doi.org/10.1016/j.apenergy.2011.03.031. <http://www.sciencedirect.com/science/article/pii/S0306261911002017>.

[16] R.J. Braun, S. Kameswaran, J. Yamanis, E. Sun, Highly efficient IGFC hybrid power systems employing bottoming organic rankine cycles with optional carbon capture, J. Eng. Gas Turb. Power 134 (2) (2011) 021801, http://dx.doi.org/10.1115/1.4004374.

[17] M. Li, J.D. Powers, J. Brouwer, A finite volume SOFC model for coal-based integrated gasification fuel cell systems analysis, J. Fuel Cell Sci. Technol. 7 (4) (2010) 041017, http://dx.doi.org/10.1115/1.4000687.

[18] M. Li, J. Brouwer, A.D. Rao, G.S. Samuelsen, Application of a detailed dimensional solid oxide fuel cell model in integrated gasification fuel cell system design and analysis, J. Power Sources 196 (14) (2011) 5903–5912, http://dx.doi.org/10.1016/j.jpowsour.2011.02.080. <http://www.sciencedirect.com/science/article/pii/S0378775311005076>.

[19] V. Spallina, M.C. Romano, S. Campanari, G. Lozza, A SOFC-based integrated gasification fuel cell cycle with CO_2 capture, J. Eng. Gas Turb. Power 133 (7) (2011) 071706, http://dx.doi.org/10.1115/1.4002176.

[20] T.A. Adams, P.I. Barton, High-efficiency power production from coal with carbon capture, AIChE J. 56 (12) (2010) 3120–3136, http://dx.doi.org/10.1002/aic.12230.

[21] A. Verma, A. Rao, G. Samuelsen, Sensitivity analysis of a vision 21 coal based zero emission power plant, J. Power Sources 158 (1) (2006) 417–427, http://dx.doi.org/10.1016/j.jpowsour.2005.09.015. <http://www.sciencedirect.com/science/article/pii/S0378775305013273>.

[22] E. Grol, Technical assessment of an integrated gasification fuel cell combined cycle with carbon capture, Energy Procedia 1 (1) (2009) 4307–4313, http://dx.doi.org/10.1016/j.egypro.2009.02.243, Greenhouse Gas Control Technologies 9Proceedings of the 9th International Conference on Greenhouse Gas Control

Technologies (GHGT-9), 16–20 November 2008, Washington DC, {USA} <http://www.sciencedirect.com/science/article/pii/S1876610209008868>.
[23] National Energy Technology laboratory (NETL), Integrated gasification fuel cell performance and cost assessment, Tech. rep., U.S. Department of Energy (DoE), 2009.
[24] National Energy Technology laboratory (NETL), The benefits of sofc for coal based power generation, Tech. rep., U.S. Department of Energy (DoE), 2007.
[25] National Energy Technology laboratory (NETL), Analysis of integrated gasification fuel cell plant configurations, Tech. rep., U.S. Department of Energy (DoE), 2011.
[26] J. Trembly, R. Gemmen, D. Bayless, The effect of IGFC warm gas cleanup system conditions on the gas-solid partitioning and form of trace species in coal syngas and their interactions with SOFC anodes, J. Power Sources 163 (2) (2007) 986–996, http://dx.doi.org/10.1016/j.jpowsour.2006.10.020, Selected Papers presented at the {FUEL} {PROCESSING} {FOR} {HYDROGEN} {PRODUCTION} {SYMPOSIUM} at the 230th American Chemical SocietyNational Meeting Washington, DC, USA, 28 August–1 September 2005 http://www.sciencedirect.com/science/article/pii/S0378775306020490.
[27] H. Ghezel-Ayagh, R. Way, P. Huang, J. Walzak, S. Jolly, D. Patel, M. Lukas, C. Willman, K. Davis, D. Stauffer, V. Vaysman, B. Borglum, E. Tang, M. Pastula, R. Petri, Integrated coal gasification and solid oxide fuel cell systems for centralized power generation, ECS Trans. 26 (1) (2010) 305–313, http://dx.doi.org/10.1149/1.3429002. <http://ecst.ecsdl.org/content/26/1/305.abstract>.
[28] M. Li, A.D. Rao, J. Brouwer, G.S. Samuelsen, Design of highly efficient coal-based integrated gasification fuel cell power plants, J. Power Sources 195 (17) (2010) 5707–5718, http://dx.doi.org/10.1016/j.jpowsour.2010.03.045. <http://www.sciencedirect.com/science/article/pii/S0378775310004544>.
[29] S. Rudra, J. Lee, L. Rosendahl, H.T. Kim, A performance analysis of integrated solid oxide fuel cell and heat recovery steam generator for IGFC system, Front. Energy Power Eng. China 4 (3) (2010) 402–413, http://dx.doi.org/10.1007/s11708-010-0122-x.
[30] N.S. Siefert, S. Litster, Exergy and economic analyses of advanced IGCC-CCS and IGFC-CCS power plants, Appl. Energy 107 (2013) 315–328, http://dx.doi.org/10.1016/j.apenergy.2013.02.006. <http://www.sciencedirect.com/science/article/pii/S0306261913001141>.
[31] H. Jin, E.D. Larson, F.E. Celik, Performance and cost analysis of future, commercially mature gasification-based electric power generation from switchgrass, Biofuels Bioprod. Biorefining 3 (2) (2009) 142–173, http://dx.doi.org/10.1002/bbb.138.
[32] W. Paengjuntuek, J. Boonmak, J. Mungkalasiri, Energy efficiency analysis in an integrated biomass gasification fuel cell system, Energy Procedia 79 (2015) 430–435, http://dx.doi.org/10.1016/j.egypro.2015.11.514, 2015 International Conference on Alternative Energy in Developing Countries and Emerging Economies <http://www.sciencedirect.com/science/article/pii/S1876610215022468>.
[33] P.K. Naraharisetti, S. Lakshminarayanan, I. Karimi, Design of biomass and natural gas based IGFC using multi-objective optimization, Energy 73 (2014) 635–652, http://dx.doi.org/10.1016/j.energy.2014.06.061. <http://www.sciencedirect.com/science/article/pii/S0360544214007609>.
[34] J. Sadhukhan, Y. Zhao, N. Shah, N.P. Brandon, Performance analysis of integrated biomass gasification fuel cell (BGFC) and biomass gasification combined cycle (BGCC) systems, Chem. Eng. Sci. 65 (6) (2010) 1942–1954, http://dx.doi.org/10.1016/j.ces.2009.11.022. <http://www.sciencedirect.com/science/article/pii/S0009250909008239>.
[35] Korea-ccs 2. <http://www.globalccsinstitute.com/projects/korea-ccs-2>.
[36] M.C. Bohm, H.J. Herzog, J.E. Parsons, R.C. Sekar, Capture-ready coal plants-Options, technologies and economics, Int. J. Greenhouse Gas Control 1 (1) (2007) 113–120, http://dx.doi.org/10.1016/S1750-5836(07)00033-3, 8th International Conference on Greenhouse Gas Control TechnologiesGHGT-8 <http://www.sciencedirect.com/science/article/pii/S1750583607000333>.
[37] Bloom Energy, ES-5700 Energy Server Datasheet, 2015. <http://www.bloomenergy.com/fuel-cell/es-5700-data-sheet/>.
[38] SOLIDPower, EnGen-2500 Datasheet, 2014. <http://www.solidpower.com/wp-content/uploads/2014/03/Data_Sheet_Engen2500_eng.pdf>.
[39] T.M. Gür, Comprehensive review of methane conversion in solid oxide fuel cells: Prospects for efficient electricity generation from natural gas, Prog. Energy Combust. Sci. 54 (2016) 1–64, http://dx.doi.org/10.1016/j.pecs.2015.10.004. <http://www.sciencedirect.com/science/article/pii/S0360128515300496>.
[40] E.J.O. Promes, T. Woudstra, L. Schoenmakers, V. Oldenbroek, A. Thallam Thattai, P.V. Aravind, Thermodynamic evaluation and experimental validation of 253 MW integrated coal gasification combined cycle power plant in Buggenum, Netherlands, Appl. Energy 155 (2015) 181–194, http://dx.doi.org/10.1016/j.apenergy.2015.05.006. <http://www.sciencedirect.com/science/article/pii/S0306261915005917>.
[41] J.T.G.M. Eurlings, Process performance of the SCGP at Buggenum IGCC, in: Gasification Technologies Conference, 1999.
[42] T. van der Stelt, N. Woudstra, P. Colonna, et al., Cycle-tempo: a program for thermodynamic modmodel and optimization of energy conversion systems, Delft university of Technology, The Netherlands. <http://www.asimptote.com>.
[43] P. Colonna, T. van der Stelt, Flsystems V1: A Program for the Estimation of Thermophysical Properties of Fluids, Delft university of technology, The Netherlands. <http://www.asimptote.com>.
[44] W. Traupel, Thermische turbomaschinen: thermodynamisch-stromungstechnische berechnung, fourth ed., Springer, Berlin, 2001.
[45] J.A. Miedema, Cycle; a general computer code for thermodynamic cycle computations studies of cogeneration in district heating systems (Ph.D. thesis), Delft university of technology, 1981.
[46] T. van der Stelt, N. Woudstra, P. Colonna, Cycle-Tempo: Technical Notes. <www.asimptote.com>.
[47] V. Gesellschaft, VDI Heat Atlas, second ed., Springer, 2010.
[48] M.A. Khaleel, J. Selman, Chapter 11 - cell, stack and system modelling, in: S.C. Singhal, K. Kendal (Eds.), High Temperature and Solid Oxide Fuel Cells, Elsevier Science, Amsterdam, 2003, pp. 291–331, http://dx.doi.org/10.1016/B978-185617387-2/50028-3. <http://www.sciencedirect.com/science/article/pii/B9781856173872500283>.
[49] E. Promes, T. Woudstra, L. Schoenmakers, V. Oldenbroek, A. Thallam Thattai, P. V. Aravind, Thermodynamic evaluation and experimental validation of 253 MW integrated coal gasification combined cycle power plant in Buggenum, Netherlands, Appl. Energy 155 (2015) 181–194.
[50] H. Saravanamuttoo, G. Rogers, H. Cohen, P. Straznicky, Gas Turbine Theory, sixth ed., Pearson Education Limited (Prentice Hall), 2009.
[51] R.C. Spencer, K.C. Cotton, C.N. Cannon, A method for predicting the performance of steam turbine-generators...: 16,500 kw and larger, J. Eng. Power 85 (4) (1963) 249–298, http://dx.doi.org/10.1115/1.3677341.
[52] F. Hanneman, B. Koestlin, Hydrogen and syngas combustion: pre-condition for IGCC and ZEIGCC, Siemens AG Power Generation, 2005.
[53] J. Kuhn, O. Kesler, Method for in situ carbon deposition measurement for solid oxide fuel cells, J. Power Sources 246 (2014) 430–437, http://dx.doi.org/10.1016/j.jpowsour.2013.07.106. <http://www.sciencedirect.com/science/article/pii/S0378775313013153>.
[54] J. Kuhn, O. Kesler, Carbon deposition thresholds on nickel-based solid oxide fuel cell anodes ii. steam:carbon ratio and current density, J. Power Sources 277 (2015) 455–463, http://dx.doi.org/10.1016/j.jpowsour.2014.07.084. <http://www.sciencedirect.com/science/article/pii/S0378775314011288>.
[55] T. Chen, W.G. Wang, H. Miao, T. Li, C. Xu, Evaluation of carbon deposition behavior on the nickel/yttrium-stabilized zirconia anode-supported fuel cell fueled with simulated syngas, J. Power Sources 196 (5) (2011) 2461–2468, http://dx.doi.org/10.1016/j.jpowsour.2010.11.095. <http://www.sciencedirect.com/science/article/pii/S0378775310020860>.
[56] C.W. Bale, P. Chartrand, S.A. Degterov, G. Eriksson, K. Hack, R.B. Mahfoud, J. Melancon, A.D. Pelton, S. Petersen, Factsage 6.4. <http://www.factsage.com/>.
[57] M.J. Moran, H.N. Shapiro, Fundamentals of Engineering Thermodynamics, fifth ed., John Wiley & Sons, Inc., 2006.
[58] N. Woudstra, Sustainable enegy systems: limitations and challenges based on exergy analysis (Ph.D. thesis), Delft University of Technology, 2012.
[59] G. Tsatsaronis, Definitions and nomenclature in exergy analysis and exergoeconomics, Energy 32 (4) (2007) 249–253, http://dx.doi.org/10.1016/j.energy.2006.07.002, ECOS 05. 18th International Conference on Efficiency, Cost, Optimization, Simulation, and Environmental Impact of Energy Systems ECOS 05 http://www.sciencedirect.com/science/article/pii/S0360544206001824.
[60] Asimptote, Cycle-tempo 5 technical notes, Tech. rep., ASIMPTOTE, 2014.
[61] H.D. Baehr, Verbrennungsprozesse, Springer Berlin Heidelberg, Berlin, Heidelberg, 1966, pp. 321–359, http://dx.doi.org/10.1007/978-3-642-53398-3_8.
[62] C.-C. Cormos, A.-M. Cormos, S. Agachi, Power generation from coal and biomass based on integrated gasification combined cycle concept with pre- and post-combustion carbon capture methods, Asia-Pacific J. Chem. Eng. 4 (6) (2009) 870–877, http://dx.doi.org/10.1002/apj.354.
[63] C.-C. Cormos, Integrated assessment of IGCC power generation technology with carbon capture and storage (CCS), Energy 42 (1) (2012) 434–445, http://dx.doi.org/10.1016/j.energy.2012.03.025, 8th World Energy System Conference, {WESC} 2010 <http://www.sciencedirect.com/science/article/pii/S0360544212002162>.